


Physical volcanology and geochemistry of Palaeoarchaeon komatiite lava flows from the western Dharwar craton, southern India: implications for Archaean mantle evolution and crustal growth

M. Jayananda, R.A. Duraiswami, K.R. Aadhiseshan, R.V. Gireesh, B.C. Prabhakar, Kowe-u Kafo, Tushipokla & R. Namratha

To cite this article: M. Jayananda, R.A. Duraiswami, K.R. Aadhiseshan, R.V. Gireesh, B.C. Prabhakar, Kowe-u Kafo, Tushipokla & R. Namratha (2016): Physical volcanology and geochemistry of Palaeoarchaeon komatiite lava flows from the western Dharwar craton, southern India: implications for Archaean mantle evolution and crustal growth, International Geology Review, DOI: [10.1080/00206814.2016.1172350](https://doi.org/10.1080/00206814.2016.1172350)

To link to this article: <http://dx.doi.org/10.1080/00206814.2016.1172350>

 View supplementary material 

 Published online: 21 Apr 2016.

 Submit your article to this journal 

 Article views: 49

 View related articles 

 View Crossmark data 

Physical volcanology and geochemistry of Palaeoarchaean komatiite lava flows from the western Dharwar craton, southern India: implications for Archaean mantle evolution and crustal growth

M. Jayananda^a, R.A. Duraiswami^b, K.R. Adhishesan^c, R.V. Gireesh^d, B.C. Prabhakar^e, Kowe-u Kafo^c, Tushipokla^{ibc} and R. Namratha^e

^aCentre for Earth and Space Sciences, University of Hyderabad, Hyderabad, India; ^bDepartment of Geology, Savitribai Phule Pune University, Pune, India; ^cDepartment of Geology, University of Delhi, Delhi, India; ^dDepartment of Geology, School of Earth Sciences, Central University of Karnataka, Kalaburagi, India; ^eDepartment of Geology, Bangalore University, Bangalore, India

ABSTRACT

Palaeoarchaean (3.38–3.35 Ga) komatiites from the Jayachamaraja Pura (J.C. Pura) and Banasandra greenstone belts of the western Dharwar craton, southern India were erupted as submarine lava flows. These high-temperature (1450–1550°C), low-viscosity lavas produced thick, massive, polygonal jointed sheet flows with sporadic flow top breccias. Thick olivine cumulate zones within differentiated komatiites suggest channel/conduit facies. Compound, undifferentiated flow fields developed marginal-lobate thin flows with several spinifex-textured lobes. Individual lobes experienced two distinct vesiculation episodes and grew by inflation. Occasionally komatiite flows form pillows and quench fragmented hyaloclastites. J.C. Pura komatiite lavas represent massive coherent facies with minor channel facies, whilst the Banasandra komatiites correspond to compound flow fields interspersed with pillow facies. The komatiites are metamorphosed to greenschist facies and consist of serpentine-talc ± carbonate, actinolite-tremolite with remnants of primary olivine, chromite, and pyroxene. The majority of the studied samples are komatiites (22.46–42.41 wt.% MgO) whilst a few are komatiitic basalts (12.94–16.18 wt.% MgO) extending into basaltic (7.71 – 10.80 wt.% MgO) composition. The studied komatiites are Al-depleted Barberton type whilst komatiite basalts belong to the Al-undepleted Munro type. Trace element data suggest variable fractionation of garnet, olivine, pyroxene, and chromite. Incompatible element ratios (Nb/Th, Nb/U, Zr/Y, Nb/Y) show that the komatiites were derived from heterogeneous sources ranging from depleted to primitive mantle. CaO/Al₂O₃ and (Gd/Yb)_N ratios show that the Al-depleted komatiite magmas were generated at great depth (350–400 km) by 40–50% partial melting of deep mantle with or without garnet (majorite?) in residue whilst komatiite basalts and basalts were generated at shallow depth in an ascending plume. The widespread Palaeoarchaean deep depleted mantle-derived komatiite volcanism and sub-contemporaneous TTG accretion implies a major earlier episode of mantle differentiation and crustal growth during ca. 3.6–3.8 Ga.

ARTICLE HISTORY

Received 24 September 2015
Accepted 26 March 2016

KEYWORDS

Komatiite; geochemistry; physical volcanology; lava flows; spinifex; emplacement dynamics; mantle plume and Archaean

1. Introduction

Komatiites are MgO-rich (>18 wt.%) ultra-high-temperature, low-viscosity lava flows mostly restricted to Archaean greenstone belts (Arndt *et al.* 2008). They are often considered to be windows to secular development of dynamic mantle (Mole *et al.* 2014) and are fundamental to our understanding of the thermal, chemical, and tectonic evolution of the early Earth. Since the discovery of komatiites in South Africa (Viljoen and Viljoen 1969), numerous studies conducted on komatiites from southern Africa, Canada, Australia, India, Finland, and Brazil (Jahn *et al.* 1980, 1982; Barnes *et al.*

1988; Arndt 1994; Hill *et al.* 1995; Lesher and Arndt 1995; Fan and Kerrich 1997; Grove *et al.* 1997; Parman *et al.* 1997; Polat *et al.* 1999; Polat and Kerrich 2000; Chavagnac 2004; Barnes 2006b; Arndt *et al.* 2008; Jayananda *et al.* 2008; Dostal and Mueller 2012; Furnes *et al.* 2013; Maier *et al.* 2013), together with experimental works (Ohtani *et al.* 1989; Herzberg and O'Hara 1998), have greatly contributed to our understanding of the origin of both komatiite magmas and Archaean mantle. However, the tectonic context of magma generation and eruption of komatiite magmas is still not fully resolved (Polat *et al.* 1999; Arndt 2003; Parman *et al.* 2004; Arndt *et al.* 2008) although most workers

CONTACT M.Jayananda ✉ mjayan.geol@gmail.com Centre for Earth and Space Sciences, University of Hyderabad, Hyderabad, India

 Supplemental data for this article can be accessed here.

© 2016 Informa UK Limited, trading as Taylor & Francis Group

consider komatiite magmas to have originated from anomalously hot mantle upwellings (Nesbit *et al.* 1993, Herzberg 1995; Arndt *et al.* 2008), probably analogous to modern mantle plumes.

In the western Dharwar craton of southern India, well-preserved komatiites have been documented from older Sargur Group greenstone belts (Naqvi 1981; Srikantia and Bose 1985; Charan *et al.* 1988; Srikantia and Venkataramana 1989; Srikantia and Rao 1990; Venkata Dasu *et al.* 1991; Devapriyan *et al.* 1994; Subba Rao and Naqvi 1999; Paranthaman 2005) and more recently minor komatiite volcanics, documented from the Bababudan Group, belong to the younger Dharwar Supergroup (Manikyamba *et al.* 2013). Most of the earlier contributions document field description of komatiites including their structure, stratigraphic relationships, and petrographic characteristics. Recent Sm–Nd whole-rock isochrons on komatiites in the central part of the western Dharwar craton reveal ages ranging from ca. 3.38–3.15 Ga (Jayananda *et al.* 2008; Mondal *et al.* 2008; Maya *et al.* 2011). Whole-rock geochemical data and Nd isotopes reveal their derivation from heterogeneous mantle sources from different depths (Jayananda *et al.* 2008; Mukherjee *et al.* 2010; Tushipokla and Jayananda 2013; Manikyamba *et al.* 2014b). However, integrated studies involving the combined physical volcanology and geochemistry of komatiites to evaluate the emplacement dynamics of lava flows and chemical and thermal evolution of source mantle havenot yet elucidated sufficient detail. Consequently, the main purpose of this contribution is to present field relationships, petrographic characteristics, and whole-rock geochemical data for the komatiite flows from the Sargur Group Jayachamaraja Pura (J.C.Pura) and Banasandra greenstone belts in the western Dharwar craton to constrain their physical volcanology and petrogenesis, including mantle evolution and the geodynamic context of komatiite volcanism.

2. Regional geological framework

The Dharwar craton (Figure 1) is a composite Archaean protocontinent comprising several crustal blocks with distinct thermal records and accretionary histories which amalgamated into cratonic framework ca. 2.5 Ga (Peucat *et al.* 2013; Jayananda *et al.* 2013a; Santosh *et al.* 2015). The craton exposes a large tilted section of continental crust offering excellent opportunities to study crustal accretion patterns along different crustal levels in three dimensions (Chardon *et al.* 2008, 2011). The Dharwar craton comprises highly voluminous TTG-type gneisses (regionally known as peninsular gneisses), two-generation volcanic-sedimentary greenstone

sequences, and late calc-alkaline to potassic plutons (Swami Nath and Ramakrishnan 1981). The craton has been divided into two major crustal blocks (western and eastern Dharwar) based on crustal thickness, thermal records, ages of the basement, and degree of melting of basement TTG (Swami Nath *et al.* 1976; Rollinson *et al.* 1981; Jayananda *et al.* 2006; Chardon *et al.* 2008). The steep mylonitic zone along the eastern boundary of the Chitradurga greenstone belt (see Figure 1) was considered as the dividing line between two crustal blocks (Swami Nath and Ramakrishnan 1981). The western Dharwar craton preserves 3.4–3.2 Ga TTG (Jayananda *et al.* 2015) and the associated Sargur Group greenstone belts with ca. 3.38–3.15 Ga volcanic sequences and inter-layered sediments (quartzite-pelite-carbonate), indicating detrital zircon ages as old as 3.6 Ga for their provenance (Meen *et al.* 1992; Nutman *et al.* 1992; Peucat *et al.* 1993; Bhaskar Rao *et al.* 2008; Jayananda *et al.* 2008). The TTG and associated Sargur Group greenstone sequences form a basement for the younger 2.91–2.67 Ga Dharwar Supergroup greenstone sequences forming the Bababudan–Chitradurga and Shimoga–Dharwar basins (Kumar *et al.* 1996; Nutman *et al.* 1996; Trendall *et al.* 1997; Jayananda *et al.* 2013b; Manikyamba *et al.* 2014a, 2014b). Several late 2.62–2.60 Ga potassic plutons intrude the basement, as well as greenstone sequences forming the terminal magmatic event and reworking corresponding to cratonization of Archaean crust in the western Dharwar craton (Bhaskar Rao *et al.* 1992; Jayananda *et al.* 2006, 2015; Chadwick *et al.* 2007; Sarma *et al.* 2012; Ram Mohan *et al.* 2014). On the other hand, the eastern block comprises large remnants/discontinuous exposures of 3.23–3.0 Ga migmatitic TTG with interlayered high-grade supracrustal rocks (quartzite-pelite-calc-silicate-manganiferous marble-BIFs), abundant 2.7–2.54 Ga tonalitic to granodioritic gneisses, 2.5–2.54 Ga volcanic dominated greenstone sequences, and highly voluminous 2.56–2.52 Ga calc-alkaline to potassic plutons (Balakrishnan and Rajamani 1987; Balakrishnan *et al.* 1990, 1999; Peucat *et al.* 1993, 2013; Jayananda *et al.* 1995, 2000, 2013a, 2013b; Chadwick *et al.* 2000; Chardon *et al.* 2002, 2011; Anand and Balakrishnan 2010; Bidyananda *et al.* 2011; Manikyamba and Kerrich 2012). More recently, based on zircon ages and Nd isotope data, three age provinces (western, central, and eastern blocks) have been identified (Dey 2013; Peucat *et al.* 2013; Jayananda *et al.* 2013a). The western block comprises the oldest TTG basement (3.4–3.2 Ga) interlayered with 3.38–3.2 Ga sequences, whilst the central block comprises a mixture of old and young TTG basement (3.38–3.0 and 2.7–2.56 Ga) with remnants of old greenstone sequences and the eastern block contains a young (2.7–2.53 Ga) tonalitic to granodioritic

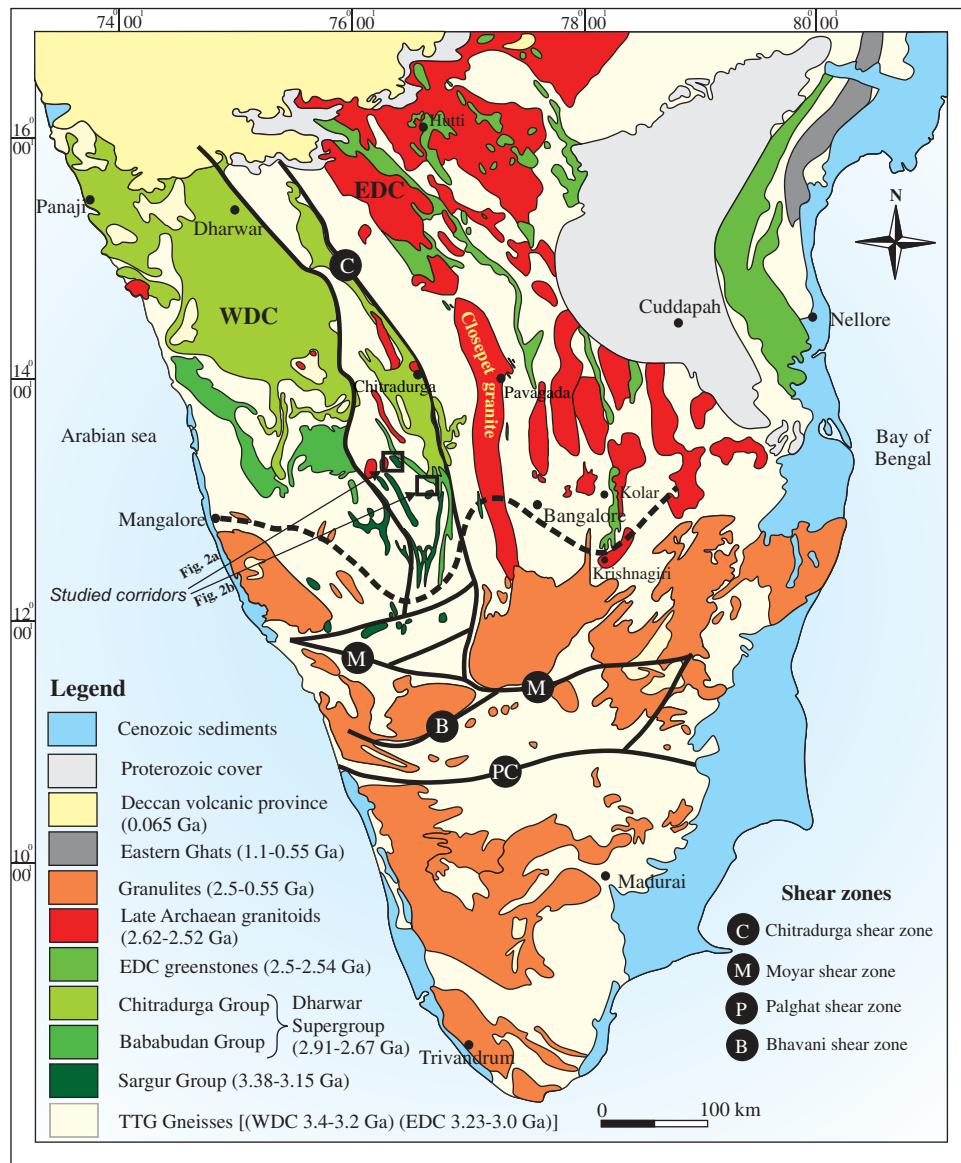


Figure 1. Geological sketch map of southern India (modified after Geological Survey of India – project vasundara) showing the studied corridors (2a and 2b). EDC, eastern Dharwar craton; WDC, western Dharwar craton.

basement with highly voluminous diatexites (Jayananda *et al.* 2013a; Peucat *et al.* 2013; references therein). The whole craton was affected by a major shear deformation during the end of the Archaean, which is sub-contemporaneous with emplacement of juvenile calc-alkaline plutons in the eastern Dharwar craton (Bouhallier *et al.* 1995; Chadwick *et al.* 2000; Chardon and Jayananda 2008; Chardon *et al.* 2008, 2011). The entire Archaean crust of the Dharwar craton was affected by a major thermal event under green schist to granulite facies conditions close to 2.5 Ga (Peucat *et al.* 1993, 2013; Jayananda *et al.* 2013a). However, texturally controlled *in situ* monazite ages and discordant zircon ages suggest pre-2.5 Ga high-temperature thermal events of granulite facies or UHT

conditions at 2.62 Ga and 3.1 Ga (Jayananda *et al.* 2011, 2013a).

3. Geological setting

In the western Dharwar craton the Sargur Group greenstone belts contain well-preserved volcanic sequences including ultramafic-mafic rocks with rare felsic volcanic sequences. The ultramafic-mafic sequences belong to komatiite-tholeiite lineage whilst the felsic volcanics corresponds to calc-alkaline lineage. In this study we focused on J.C. Pura and Banasandra greenstone sequences (see Figure 1), which stratigraphically underlie the Kibbanahalli arm (Figure 2) of the Bababudan Group

Stratigraphic successions of Sargur Group-JC Pura and Banasandra greenstone belt (Venkata Dasu et al., 1991; Srikantia and Bose, 1985; Jayananda et al., 2008; Maya et al., 2011)		
	JC Pura	Banasandra
Dharwar Supergroup	Amygdular metabasalt closely inter-bedded with cross-bedded and ripple marked quartzite quartz-biotite-chlorite-garnet schist	Metabasalts/amphibolites
Bababudan Group (Gibbanahalli arm)	Oligomict conglomerate	Conglomerate/quartzites
	Unconformity	Unconformity
	Peninsular gneisses (3.30 Ga)	
Sargur Group	Ultramafic/mafic rocks with interlayered chert/quartzite (3.38 Ga)	Ultramafic rocks (3.35 Ga)
	Oldest Archean basement? (> 3.4 Ga)	Old Archean basement (> 3.4 Ga?)

Figure 2. Stratigraphic successions of Sargur Group – J.C. Pura and Banasandra greenstone belt (Venkata Dasu *et al.* 1991; Srikantia and Bose 1985; Jayananda *et al.* 2008; Maya *et al.* 2011).

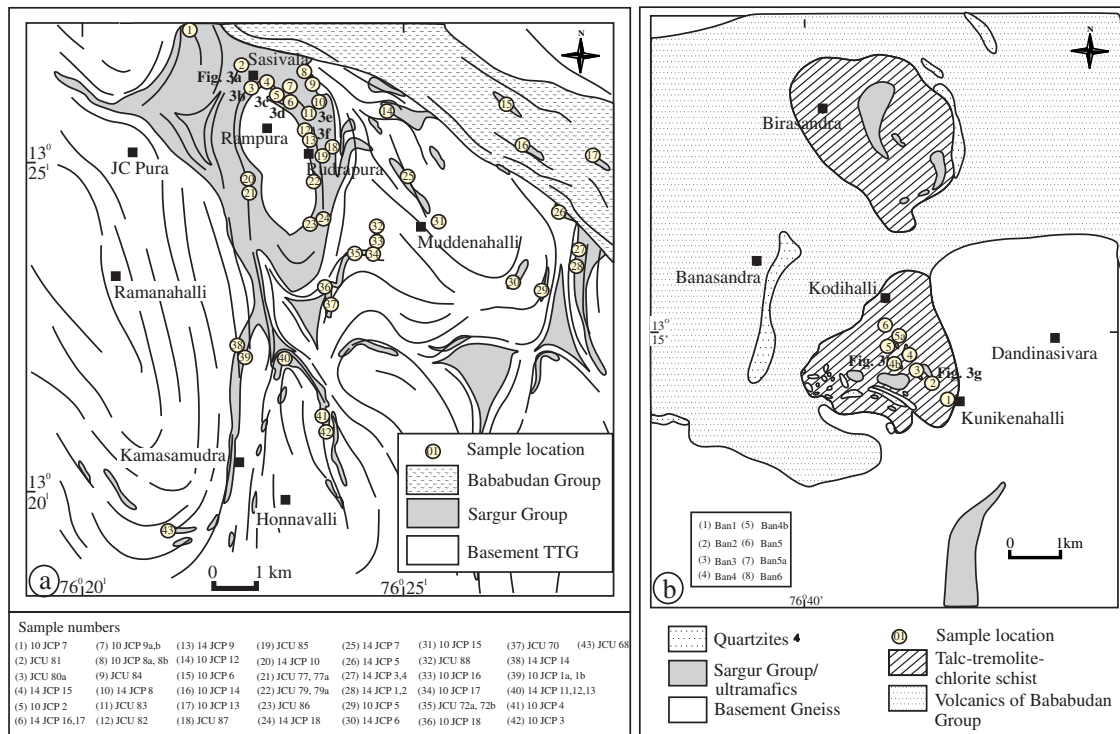


Figure 3. (a) Geological sketch map of J.C. Pura (3.38 Ga) greenstone belt (Venkata Dasu *et al.* 1991; Chardon *et al.* 1996) showing sample locations. (b) Geological map of Banasandra (3.15 Ga) greenstone belt (Srikantia and Bose 1985) showing sample locations.

belonging to the Dharwar Supergroup (Venkata Dasu *et al.* 1991; Ramakrishnan *et al.* 1994; Chardon *et al.* 1996).

3.1. J.C.Pura greenstone belt

The J.C. Pura belt is an oval-shaped volcanic-sedimentary greenstone basin located in the northwestern part of the Kibbanahalli arm (Figure 3(a)), which

is dominated by massive to schistose komatiitic volcanic rocks. Detailed lithological mapping, stratigraphic relationships, and structural analysis were documented by Venkata Dasu *et al.* (1991) and Chardon *et al.* (1996). A pronounced stratigraphic break between the J.C. Pura belt (older Sargur Group) and Kibbanahalli arm (younger Bababudan Group) volcanic-sedimentary sequences has been demonstrated through unconformity defined by

oligomict quartz-pebble conglomerate (Venkata Dasu *et al.* 1991). The J.C. Pura greenstone belt comprises voluminous ultramafic (komatiite and komatiitic basalts) with minor mafic rocks (basaltic), cherty quartzites, and minor BIFs. The komatiites are represented by greyish-green ultramafic rocks including fine- to medium-grained serpentinites, serpentine-talc-tremolite, tremolite-actinolite, and talc-chlorite schists. Numerous tiny (width 0.5–1 cm) carbonate veins traverse the komatiites. Isolated thin discontinuous cherty quartzite bands are found in association with greenstone volcanics. Single zircon evaporation ages indicate 3.23 Ga for their provenance (Ramakrishnan *et al.* 1994). Komatiites display spectacular pillows (diameter 5–20 cm), pillow breccias and flow top breccias with chilled margins. Crude spinifex textures are also documented in ultramafic komatiite (Venkata Dasu *et al.* 1991; Prabhakar and Namratha 2014). Komatiites also show polyhedral jointing, vesicular, nodular, and ocelli structures (Venkata Dasu *et al.* 1991; Jayananda *et al.* 2008).

3.2. Banasandra greenstone belt

The Banasandra greenstone belt is exposed in the southeastern part of the Kibbanahalli arm (see Figure 3(b)) of the Chitradurga belt. The greenstone belt forms a thin NNW-trending belt as well as sporadic outcrops around Kunikenahalli and Kodihalli south of Banasandra. This belt comprises massive fine-grained ultramafic rocks comprising massive serpentinites, pillowed to spinifex-textured komatiites, and minor amphibolites (Srikantia and Bose 1985; Jayananda *et al.* 2008). Spectacular spinifex-textured komatiites are located about 0.5 km south of Kodihalli, with criss-crossing sheaves of closely spaced olivine (now serpentine) needles measuring 3–10 cm in length. Among the exposures displaying spinifex textures, a gradation from larger needles at the lower levels to smaller needles at higher levels is observed. Fine-grained pillowed or brecciated lava flows are confined to the southern part of the Banasandra belt exposed at the northwestern outskirts of Kunikenahalli village. These pillowed komatiites are considered to underlie the spinifex-textured komatiites (Srikantia and Bose 1985).

3.3. Physical volcanology

The komatiite flows from the present study show characteristics akin to undifferentiated massive lava flows, with polyhedral joints and fully differentiated lava flows with a spinifex-textured upper layer and

olivine cumulate lower layers (Pyke *et al.* 1973; Arndt *et al.* 1977). Rare pillowed units and various types of fragmental komatiite are also present (Arndt *et al.* 2008). The komatiite lavas were studied from five locations in and around Rampura, while those from Banasandra were studied from two locations near Kunikenahalli (Figure 3(b)). The J.C. Pura komatiite lavas are simple, massive units that are sporadically topped by flow top breccias. In contrast, the komatiite lavas from Banasandra are thin, compound, and pillowed with a predominance of quench shattered hyaloclastites. Individual lava units exhibit well-developed internal spinifex zonations. Most J.C. Pura komatiite lavas represent a predominant massive coherent facies with minor conduit/channel facies, while the Banasandra komatiite lavas represent a large compound flow field with sheet flow facies interspersed with pillow facies.

3.3.1. Physical volcanology of the J.C. Pura komatiites

Massive undifferentiated komatiite lava flows are most common as prominent resistant ridges in the Rampura area, making up to 60% of the hill sections (Hill *et al.* 1995; Dann 2000). The komatiite lava flows vary in thickness from 2 to 15 m while their basaltic komatiite counterparts are even thicker (20–30 m). These lava flows occur as long drawn lobes and lava sheets spread over 10–50 m in length. The komatiite lavas are serpentinized, but at places relict olivine are seen. Equant, euhedral crystals of chromite are seen in the serpentinized pyroxene–glass matrix.

Two prominent hill ranges on the Sasivala–Rampura road expose a 70–90 m-thick sequence of komatiite lavas (Figure 4(a,b)). The lowermost ~25 m of the first hill section exposes chlorite schist formed due to low-grade metamorphism of the komatiite. Chlorite schist often forms from metamorphism of A-zone komatiites due to lower MgO and a higher proportion of evolved trapped liquid (David Mole, pers. comm.). An ~20 m-thick massive komatiite lava flow contains spherical structures that range in diameter from 3 to 5 mm (Figure 5(a)). These have been referred to as ‘ocelli’ by Venkata Dasu *et al.* (1991). The spherical structures occur either as irregular patches within the serpentinized lava flow or as continuous distinct bands towards the top. Petrographically the spherical structures are formed of pyroxene–glass aggregates. These are fairly resistant to weathering in comparison to the serpentinized matrix, and form knobby protrusions on the surface of the rock (Figure 5(b)). Large (5–10 mm) undeformed spherical knobs are also seen in other massive komatiite lavas higher up in the section, but the frequency of the knobs is low in comparison to

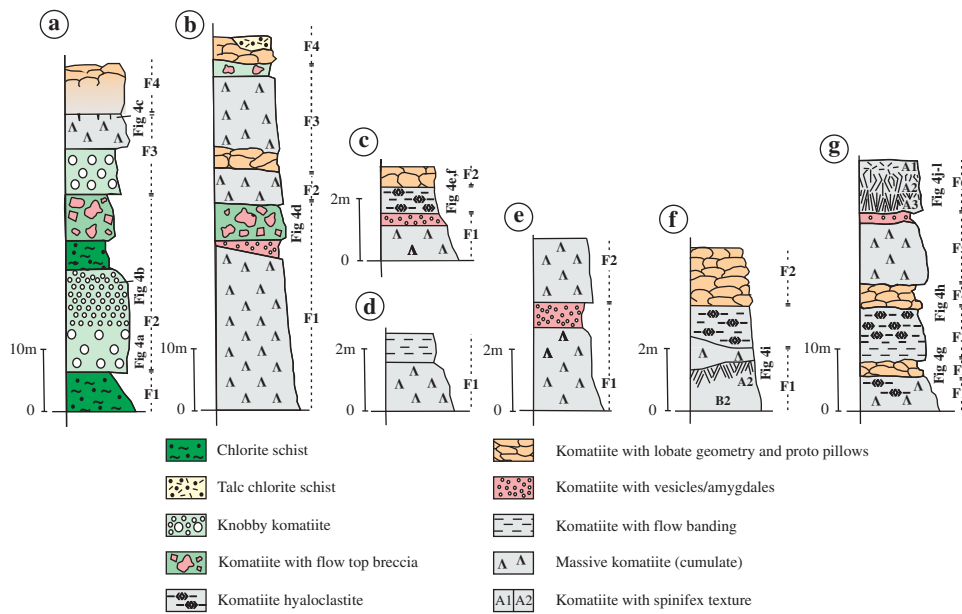


Figure 4. Lithologs of komatiites from (a–e) Rampura section in J.C. Pura greenstone belt and (f–g) Kunikenahalli–Kodihalli section of Banasandra greenstone belt.

those exposed in the lower lava flows. The lower part of the komatiite lava flows exposed at the base of the section is also characterized by large (>1 cm), deformed knobby komatiite that has been metamorphosed to chlorite schist. Individual knobs are augen-shaped and are aligned parallel to the foliation.

The occurrence of vesicular komatiite is sparse in the studied komatiite lava flows, but a few sporadic and laterally discontinuous examples can be seen in and around Rampura (Figure 4(b, c, e)). The importance and significance of vesicle distribution was realized after these were observed at three to four separate vesicle-rich levels within thick komatiite lava flows at Kambalda, Western Australia (Beresford *et al.* 2000). The vesicle layers are not separated by glassy margins or partings and were considered to represent multiple lava pulses, suggesting an incremental emplacement by endogenous growth. The vesicles from the Rampura komatiite are small, spherical, and generally range in size from 0.5 to 1 cm. Many vesicles tend to coalesce and form elliptical, interconnected patterns. In the Rampura komatiite lava flows the vesicular horizons are mostly found towards the flow top but in some lava flows the vesicles tend to accumulate towards the middle of the thick lava flows.

The original surfaces of the komatiite flows are not preserved, but wherever exposed, they show a smooth surface with a few shallow dipping cracks resembling inflation clefts. The komatiite lava flows are conspicuous by the absence of regular cooling

joints perpendicular to cooling surfaces, but the flows are characterized by the presence of various patterned polygonal joints (Figure 5(c)). Small outcrops and blocks preserving polygonal joints are exposed at several places, suggesting that these were derived from the upper parts of the komatiite lava flow. Most komatiite lava flows around Rampura show sporadic and patchy occurrences of fragmental komatiite (Figure 5(d)). We refer to these as *in situ* products of mechanical disintegration (autobrecciation) of a previously intact komatiite crust formed during flowage. The term ‘flow top breccias’ is used by us to distinguish them from those produced due to quench fragmentation processes. The fragmental flow top breccias form due to break-up and ‘tearing’ of the flow top crust due to rapid flow of lava beneath the crust. Two prominent horizons of fragmental komatiite are exposed (Figure 4(a,b)) in the hill ridges west of Rampura. Here, the flow top breccias consist of 5–14 cm-wide angular to sub-angular fragments; individual fragments are displaced relative to each other. The fragments on the komatiite flow are highly oxidized, glassy, and constitute a monomict breccia. However, some vesicular fragments are also seen. The flow top breccia on komatiite lava flows from J. C. Pura developed due to auto-brecciation of flow tops due to high strain rates, in response to high effusion rates and rapid cooling.

Prominent horizons of fine komatiite hyaloclastite are seen in the ridges on the way to Rampura (Figure 4(c)). The hyaloclastites are heterogeneously distributed over

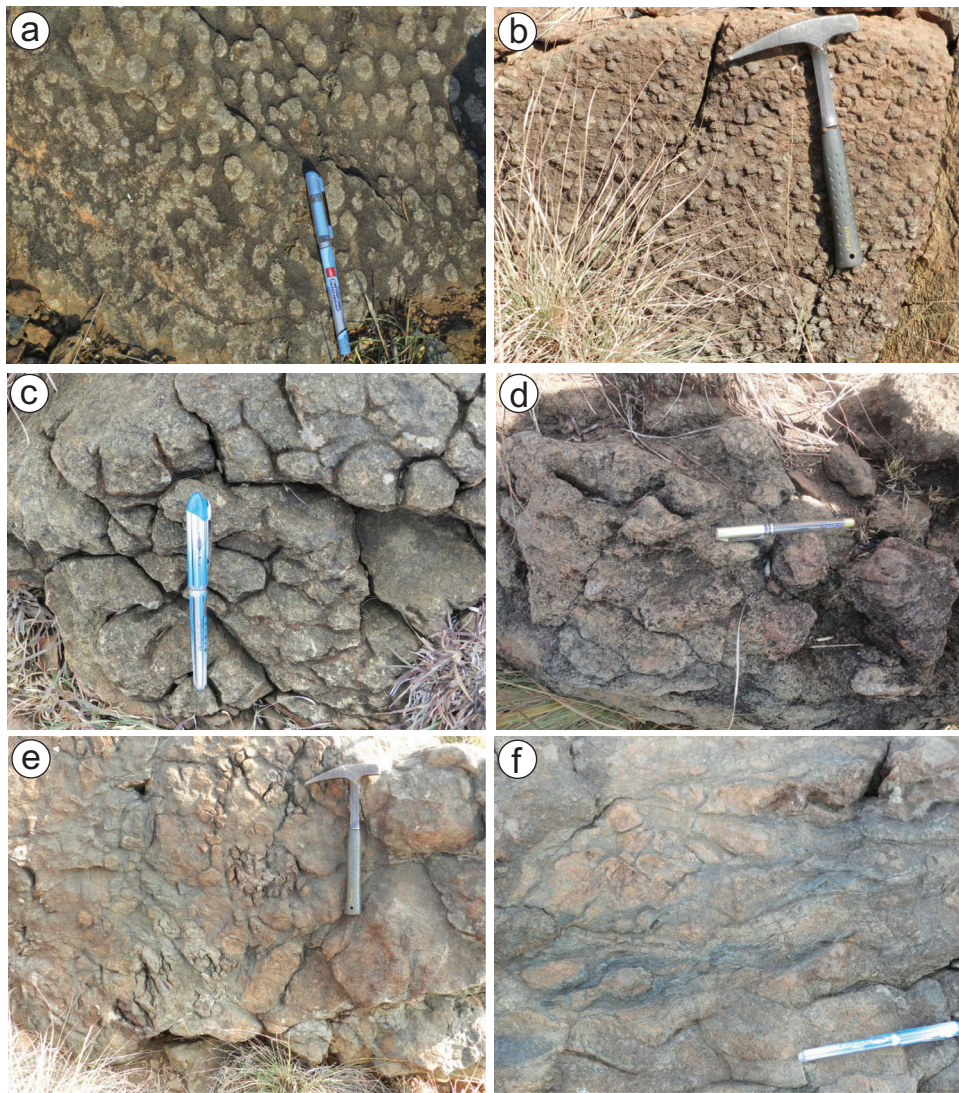


Figure 5. Field photos of komatiites from J.C. Pura: (a) spherical knobs of pyroxenes; (b) knobby komatiite resistant to weathering; (c) polysutured top of a komatiite lava flow; (d) flow top breccia formed due to mechanical disintegration of top of komatiite lava; (e) craggy hyaloclastite formed due to quench fragmentation of komatiite lava with sea water; (f) flow rafted hyaloclastite fragments in komatiite lavas. Field photos of komatiites from Banasandra (Kunikenahalli–Kodihalli section): (g) spherical bulbous pillows at the base of massive komatiite lavas; (h) elongated pillows extruded from a massive komatiite mound; (i) compound komatiite showing contact between massive cumulate of upper lobe and the spinifex zones of the lower lobe; (j) contact between A1 (random spinifex) and A3 (platy spinifex) zones; (k) chevron spinifex in the A-zone of a komatiite lobe; (l) fine acicular spinifex texture.

pillows and komatiite sheets. Besides this, komatiite hyaloclastite also occurs within cracks and crevices. The komatiite hyaloclastite contains 2–5 cm-wide clasts set in a finer matrix (Figure 5(e)). Fragments constituting the hyaloclastite are unsorted and consist of angular to sub-angular glassy and altered komatiite. The komatiite hyaloclastite also shows flowage of rafted clasts (Figure 5(f)). The hyaloclastites form due to quench fragmentation of hot komatiite lavas in contact with seawater. Occasionally, hyaloclastite which forms at the top of erupting lava flows was incorporated into the hot and highly fluid komatiite lava streams or hose-like ejections, producing the fluidal rafted clasts.

3.3.2. Physical volcanology of the Banasandra komatiites

At Kunikenahalli, around 15% of komatiite flows are spinifex-textured, 20% are pillowed, 15% are fragmental hyaloclastites, 5% are vesicular, while the remaining 45% are massive, undifferentiated, and are similar to those reported for the Barberton greenstone belt (Dann 2000). In the section beside the canal near Kunikenahalli (Figure 4(f)), massive komatiite with well-developed polygonal cracks is exposed at the base and is followed by a prominent horizon of hyaloclastite with preserved traces of flowage of rafted fragments. Komatiite with lobate geometry and curved cracks is

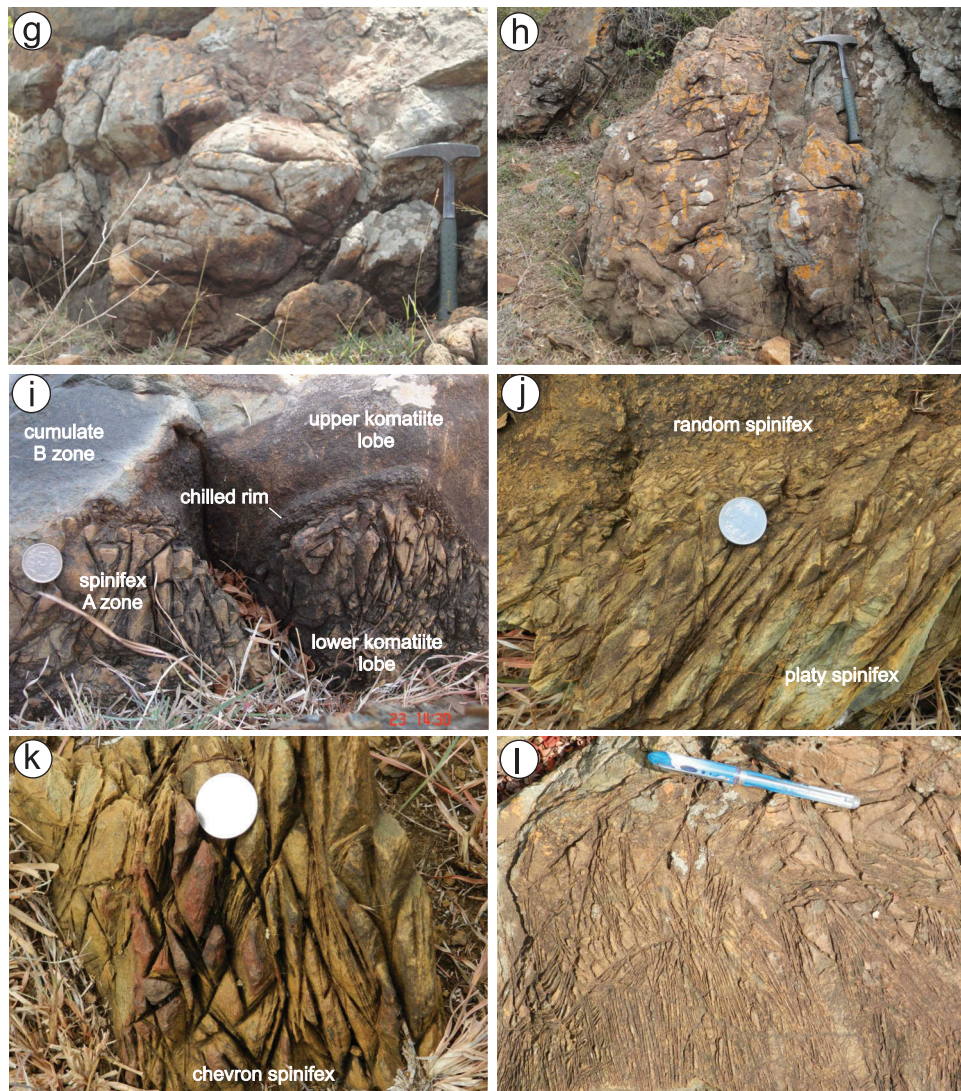


Figure 5. (Continued).

common in the upper parts of the section. Many such curved cracks are related to cooling and produce rounded to elongated enclaves of massive komatiites. These were previously interpreted as pillows (e.g. Figure 4, D-18 of Ramakrishnan and Vaidyanadhan 2008).

Mounds of pillowed komatiite lava are seen at the base of the hills besides the temple near Kunikenahalli (Figure 5(g)). Most proto pillows studied from the Kunikenahalli section are characterized by smooth surfaces and are devoid of vesicles. We prefer to call these proto pillows as their distinctive internal structure is not as well developed as in basaltic pillows from the younger greenstone belts in southern India (Duraiswami *et al.* 2013). Small elongated, smooth-surfaced, proto pillows occur in clusters in a manner suggesting that they emanated from the top of a mound (Figure 5(h)). In places,

stacks of small, rounded to bulbous proto pillows or elongated proto pillows with radial cracks and few vesicles are exposed in cross-section. Occurrences of lobate or tongue-like pillows are also recorded from the Kunikenahalli section and are similar to those from Pyke Hill outcrops (Pyke *et al.* 1973; Shore 1996).

The komatiite lavas exposed at the base of the hills besides the temple near Kunikenahalli also expose thick horizons of hyaloclastite. In one of the low-lying outcrops (Figure 4(f)), the massive komatiite flow is overlain by an ~1.5 m-thick horizon of hyaloclastite that preserve traces of clast flowage. Most clasts in this horizon are augen shaped and aligned in a linear pattern. Large blocks of massive komatiite with different patterns of polygonal joints are seen in the Kunikenahalli section. These polygonal joints are very prominent and are enhanced due to weathering, lending exotic, curved

polygonal or hexagonal patterns to the massive flows. In some of the massive komatiite flows the polygonal joints diminish with depth and polygon joint-free zones are seen towards the mid-sections of thicker flows.

Spinifex-textured komatiite lobes are seen towards the top of the Kunikenahalli section (Figure 4(g)). Many intact and part komatiite lobes are also found as scattered outcrops on cultivable farmland. Many lobes show the development of a spinifex texture. Spinifex texture (Lewis 1971; Nesbitt 1971) is characterized by large, platy blades of olivine or acicular needles of augite formed during relatively rapid *in situ* crystallization of ultramafic or highly mafic liquids (Arndt *et al.* 2008). The A-zone of individual lobes from Kunikenahalli shows the development of spinifex textures (Figure 5(i)). Three types of spinifex texture are commonly seen to co-exist in the A-zone. The random spinifex texture (A1) is developed just below the polysutured tops of sheet lobes (Figure 5(j)), and this is followed by either the platy spinifex zone (Figure 5(j)), where plates or 'books' of olivine are roughly arranged parallel to each other, or chevron spinifex representing A2 (Figure 5(k)). Rarely, 5–15 cm-long radiating needles of olivine characterize the finer spinifex texture (Figure 5(l)). The random spinifex texture is not as common as the platy spinifex, and is characterized by small, randomly oriented olivine plates.

4. Petrography

4.1. J.C. Pura greenstone belt

The studied komatiite samples of J.C. Pura greenstone belt show diverse petrographic characteristics in regard to both texture and mineralogy. They are fine to medium grained and rarely display a coarse-grained texture. Primary mineralogy is nearly absent except in a few studied samples where remnants of either primary olivine (Figure 6(a)) or pyroxenes (Figure 6(b)) are preserved. The preserved secondary minerals developed during post-magmatic hydrothermal alteration and low-grade metamorphism under green schist to lower amphibolite facies conditions. The rocks are generally fine grained and occasionally exhibit a medium-grained texture. The common mineral assemblages observed are serpentine-talc (Figure 6(c)) and actinolite-tremolite-opaques (Figure 6(d)).

Serpentine is the most abundant mineral phase in J.C. Pura komatiites. In rare instances, remnants of pyroxene containing inclusions of serpentine can be observed. Carbonates form tiny microscopic vein networks, probably corresponding to fluid pathways.

The primary mineralogy and whole-rock chemistry have a major influence on these alteration assemblages, i.e. olivine-dominated rocks such as cumulates form serpentine and talc-rich rocks (B-zone). Rocks with less olivine and/or a greater trapped liquid component (usually more evolved) form chlorite-actinolite rocks. These assemblages are typically found in A-zone komatiites.

4.2. Banasandra greenstone belt

Ultramafic komatiites are the most dominant lithologies, showing a fine- to medium-grained texture. In some instances randomly oriented needles of olivine crystals (now serpentine) corresponding to spinifex textures are observed (Figure 6(e)).

The common mineral assemblages are talc-serpentine-tremolite ± carbonate (Figure 6(f)), with carbonates and opaques as common accessory phases. Carbonates are found as disseminated grains or occasionally form tiny venous networks.

5. Geochemistry

5.1. Major and trace elements

Major and trace element contents, together with elemental ratios of the studied volcanic sequences of J.C. Pura and Banasandra greenstone belts, are presented in supplementary table. Details of analytical procedures are presented in the Appendix. The greenstone volcanics show a wide range of elemental composition. The distinction between komatiites and komatiite basalts is mainly based on the MgO contents as defined by Arndt and Nisbet (1982). Out of the 66 samples analysed, 32 were classified as cumulate komatiites (30.7–42.4 wt.% MgO), non-cumulate komatiites (22.2–30.4%), whilst seven are komatiitic basalts (12.94–16.18 wt.% MgO) and four are basaltic (7.71–10.80 wt.% MgO) by composition. This feature is also clearly reflected in the CaO–MgO–Al₂O₃ triangular plot (Figure 7(a)) of Viljoen *et al.* (1982) and the Al₂O₃–Fe₂O₃ + TiO₂–MgO (Figure 7(b)) diagram (Jenson 1976; modified by Viljoen *et al.* 1982). On the Al₂O₃ versus FeO/(FeO + MgO) binary diagram, the samples plot in the fields of Barberton komatiite and Barberton komatiite basalt field (Figure 7(c)). Most of the studied komatiites show an Al-depleted character [CaO/Al₂O₃ = 1.66–1.03 and Al₂O₃/TiO₂ = 6.86–12.97], except for two that show an Al-non-depleted character [CaO/Al₂O₃ = 0.75–0.71 and Al₂O₃/TiO₂ = 18.53–22.47]. On the other hand, komatiite basalts display a transitional character from Al-depleted to non-depleted komatiites [CaO/Al₂O₃ = 1.30–0.77 and Al₂O₃/

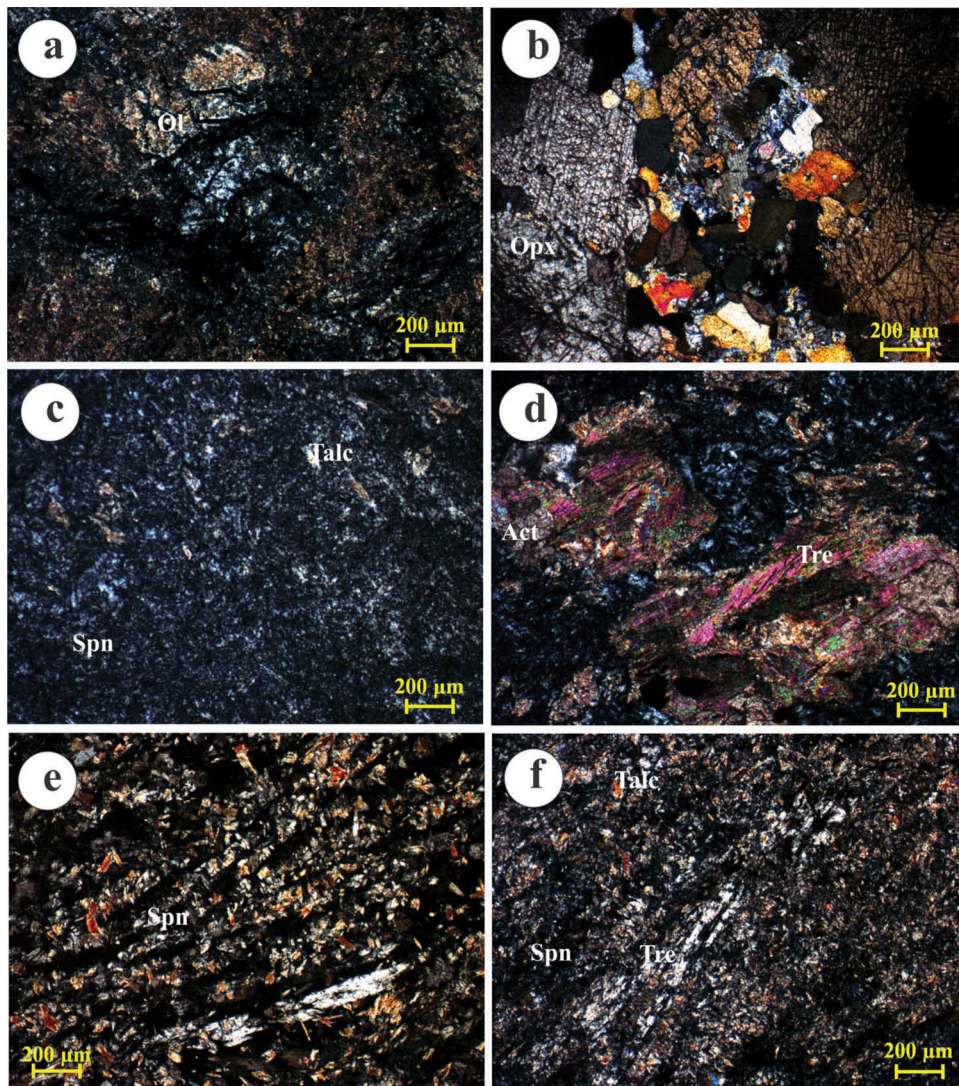


Figure 6. Photomicrographs of ultramafics showing different mineral assemblages: (a) remnant olivine grain in serpentine matrix; (b) orthopyroxene with minor olivine and serpentine; (c) serpentine-tremolite; (d) serpentine-tremolite-actinolite; (e) books of serpentinized olivine grains defining microspinel texture; (f) serpentine-talc-tremolite.

TiO₂ = 15.54–20.82]. In summary, the studied komatiites belong to the Al-depleted Barberton type whilst the majority of komatiite basalts belong to the Al-undepleted Munro type (Arndt 2003). On Harker's binary diagrams the cumulate komatiites from J.C. Pura and Banasandra form a distinct cluster. The major element oxides (Al₂O₃, TiO₂, Fe₂O₃, MnO, CaO, and Na₂O) of non-cumulate komatiites show moderate to strong negative correlation, whilst samples of komatiite basalts form separate clusters that define moderate to poor negative correlation (Figure 8(a–h)).

The komatiites and komatiitic basalts are characterized by a variable but generally high content of Ni and Cr, but conversely low Zr, Y, Sr, Th, U, Rb, and Ba (supplementary table). On Harker's binary diagrams Ni shows a positive correlation with MgO, suggesting

olivine fractionation (Figure 8(i)), whilst Cr forms clusters indicating fractionation of olivine, pyroxene, and chromite (Figure 8(j)). A large spread in Rb, Ba, and Sr (data not shown) indicate the role of secondary processes such as hydrothermal alteration.

Rare earth elements (REEs) are normalized to Leedy chondrites (Masuda *et al.* 1973) and divided by 1.2, with values of Pr, Tb, Ho, and Tm interpolated after Taylor and Gordon (1977). The komatiite samples from the present study are divided into four cumulate groups and two non-cumulate groups based on REE content, REE patterns, and Eu anomalies, whilst komatiite basalts are divided into two groups (Figure 9). The cumulate komatiites from Banasandra and J.C. Pura are characterized by high MgO content (30.7–42.4 wt. %) and exhibit flat chondritic REE patterns (Figure 9

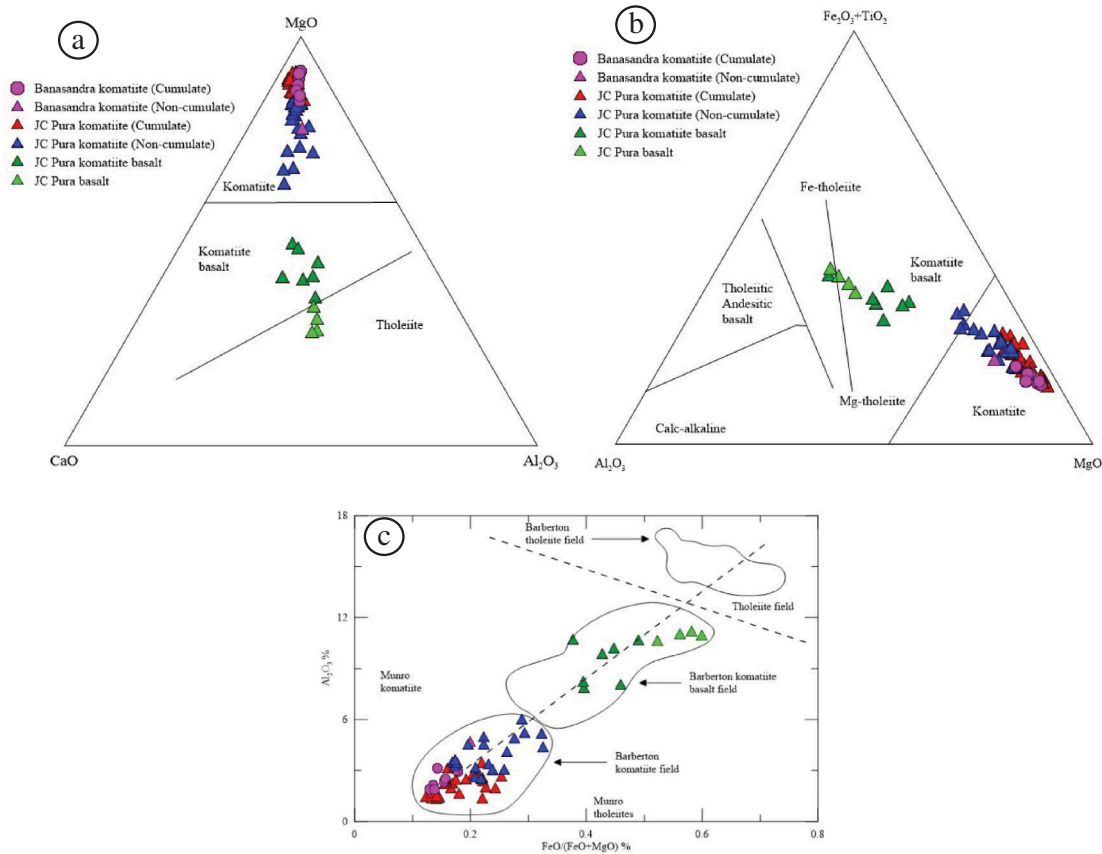


Figure 7. (a) CaO-MgO-Al₂O₃ ternary plot (Viljoen *et al.* 1982) showing cumulate, non-cumulate komatiite, and komatiite basalt composition; (b) Al₂O₃-Fe₂O₃+TiO₂-MgO ternary plot (Jenson 1976; modified by Viljoen *et al.* 1982) displaying komatiite–komatiite basalt composition; (c) FeO/(FeO+MgO) versus Al₂O₃ binary diagram showing Barberton komatiite and komatiite basalt field.

(a–d)) with low to moderate (2.31–39.63 ppm) total REE contents. The Banasandra komatiite cumulates, however, contain relatively low total REEs (4.38–12.15 ppm). The (Gd/Yb)_N ratios of all cumulates vary from 0.53 to 3.35 and their CaO/Al₂O₃ ratios vary from 0.85 to 2.92. Some cumulates from J.C. Pura exhibit a slightly enriched LREE pattern (5–10-fold) and exhibit prominent negative Eu anomalies (Eu/Eu* = 0.33–0.78). A few J.C. Pura samples also show positive Eu anomalies reflecting hydrothermal alteration (Figure 9(d)). Erratic negative and positive Eu anomalies (Figure 9(c, d)) are generally attributed to the differential mobility of Eu²⁺ relative to trivalent REEs during secondary processes such as hydrothermal alteration (Sun and Nesbitt 1978; Arndt 1994).

In comparison to the cumulates, the non-cumulate komatiites have relatively lower MgO contents (22.26–35.64 wt.%) with low to moderate total REEs (4.84–90.41 ppm). They have low (Gd/Yb)_N (0.45–1.59) and CaO/Al₂O₃ (0.70–1.64) values. Their REE patterns (Figure 9(e)) show slight LREE enrichment (4–14-fold), but many

samples are characterized by prominent negative Eu anomalies (Figure 9(f)).

The komatiite basalt-tholeiite samples have low MgO contents that vary from 7.71 to 16.18 wt.%, and moderate to high total REEs (21.66–150.37 ppm). (Gd/Yb)_N varies from 0.42 to 4.38 and CaO/Al₂O₃ varies from 0.77 to 1.30. Based on the REE patterns, these samples have been separated into two subgroups. Most samples have flat REE patterns with only a few samples showing an increase (9–30-fold) in LREE content (Figure 9(g)). Two samples (JCU 81, 10JCP6), however, show high total REEs (105.46–150.37 ppm) and fractionated [(Gd/Yb)_N = 1.86–4.38] REE patterns (Figure 9(f)).

On the primitive mantle-normalized (Sun and McDonough 1989) multi-element plots, J.C. Pura komatiites are variable in large ion lithophile elements (LILEs), Nb, Y, and Eu contents but display uniform Pb, Zr, Hf, and Ti and a flat HREE pattern (Figure 10(a–h)). The Banasandra cumulate komatiites show a uniform pattern with slightly positive Nb anomalies, strong negative Hf anomalies, and flat HREE patterns (Figure 10(a)). The J.C.

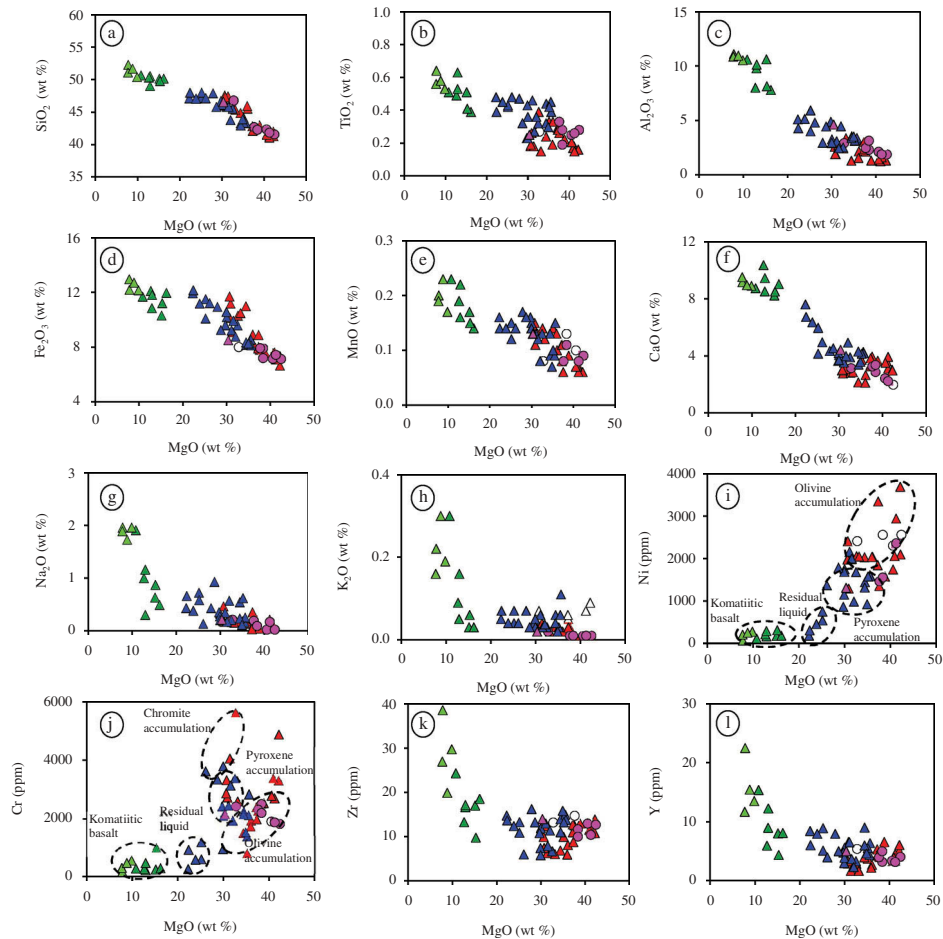


Figure 8. (a) Harker's variation diagrams for major and selected trace element showing moderate to strong fractionation trends of cumulate and non-cumulate komatiites from J.C. Pura and Banasandra greenstone belts, and komatiite basalts from J.C. Pura greenstone belt. Legends following as per Figure 7.

Pura cumulate komatiites (with low to moderate total REEs) show crossings in LILEs, slightly negative Y and Zr anomalies, but strongly negative Hf anomalies (Figure 10(b–d)). Some samples show slightly positive Nb but consistently negative Zr, Hf, and Y anomalies. In J.C. Pura cumulate komatiites, both negative (Figure 10(c)) and positive (Figure 10(d)) Eu anomalies can be seen. The non-cumulate komatiite from J.C. Pura (Figure 10(e–f)) has significantly higher HREEs (up to 9-fold) compared to its cumulate counterpart (enrichment up to two-fold), indicating significant melting of garnet in the source. The REE patterns are characterized by crossings in LILEs, and positive Nb and negative Y anomalies. One set of samples have negative Eu anomalies. The komatiitic basalt-tholeiite group (moderate to high total REEs) shows crossings in LILEs with variable (negative to positive) Nb–Hf anomalies and flat to negative Y anomalies (Figure 10(g)). Two samples (high total REEs) are characterized by variable LILEs, positive Nb, and negative Hf anomalies (Figure 10(h)).

6. Discussion

6.1. Physical volcanology and emplacement conditions

Komatiites are ultramafic lavas considered to be produced in hotspot environments during the Archaean, less frequently in Phanerozoic times (Arndt 2003). Traditionally, komatiites have been used to decipher records of thermal and chemical evolution of the mantle through time, but more recently the physical volcanology and internal structures have been used to understand their emplacement dynamics and cooling histories. The field disposition of komatiites from the J. C. Pura and Banasandra greenstone belts has been interpreted by us as resembling oceanic mounds or an oceanic komatiitic plateau above an Archaean plume. The komatiite lava flows exposed in these areas therefore exhibit submarine characters and were probably emplaced in a non-turbulent environment at high effusion rates. It is envisaged that the komatiite erupted in a

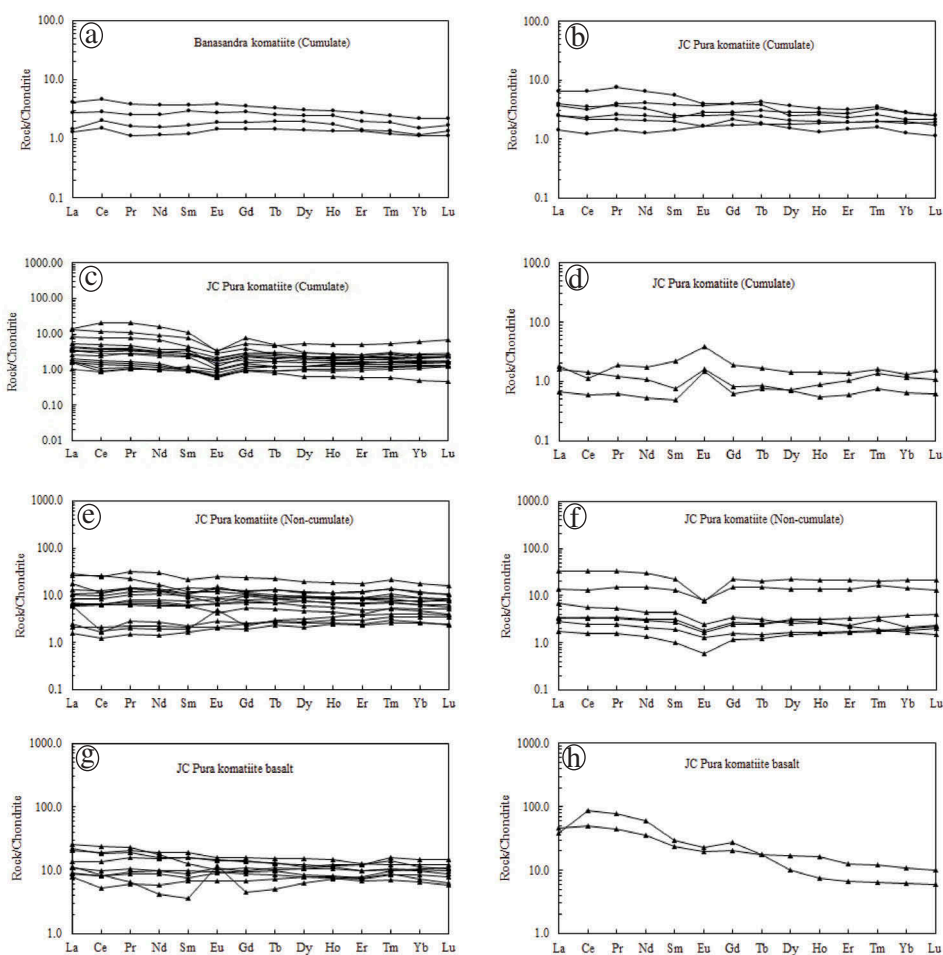


Figure 9. (a–h). Chondrite-normalized REE patterns of cumulate and non-cumulate komatiites from J.C. Pura and Banasandra, and komatiite basalts from J.C.Pura greenstone belt.

fire-fountain or hose-like ejection into seawater, and the low viscosity lavas then flowed away from the eruption locus. The massive komatiite flows from J.C. Pura are tabular with low aspect ratios (T/L 0.2–0.4), reflecting extremely low viscosity (0.1–10.0 Pas, Huppert and Sparks 1985). The low viscosity and high effusion rate enabled emplacement of these lavas over greater lateral extents compared to their basaltic counterparts. Substantially thick flows from the Rampura area accumulated large spherical pyroxene–glass structures to form ‘knobby’ komatiite similar to those found in the Pyke Hill flow (Arndt *et al.* 2008). The massive undifferentiated komatiite lava flows from J.C. Pura represent B-zones (high MgO, 30.6–42.2 wt.%) with cumulate textures. Thicker B-zones within thick, differentiated komatiites suggest a channel/conduit facies.

The substantially thick komatiite flows from J.C. Pura also show the development of a thick vesicular crust. Vesicles are generally sparse in komatiite lavas (Arndt

et al. 2004) when compared to high vesicle density in their basaltic counterparts, possibly related to the low volatile content or their accumulation and preservation in high-temperature, low-viscosity lavas. The low percentage (~1%) of vesicular komatiite in most J.C. Pura sections is similar to that reported by Dann (2001) for komatiite sequences from the Barberton Greenstone Belt. Based on the disposition of vesicular horizons, it is envisaged that at least two distinct stages of vesiculation were associated with the J.C. Pura komatiite flows. The absence of stretched and highly deformed vesicles indicates the formation of vesicles in a low-strain regime.

The presence of polysutured cracks on top of the J.C. Pura komatiite lava flows is attributed to shrinkage and cooling-induced jointing (Arndt *et al.* 2008). Significant cooling at the komatiite flow top (1000 to a few °C h⁻¹, Huppert and Sparks 1985) and rapid flow beneath the crust induced a stress regime that led to break-up and ‘tearing’ of the flow top crust to form flow top breccias.

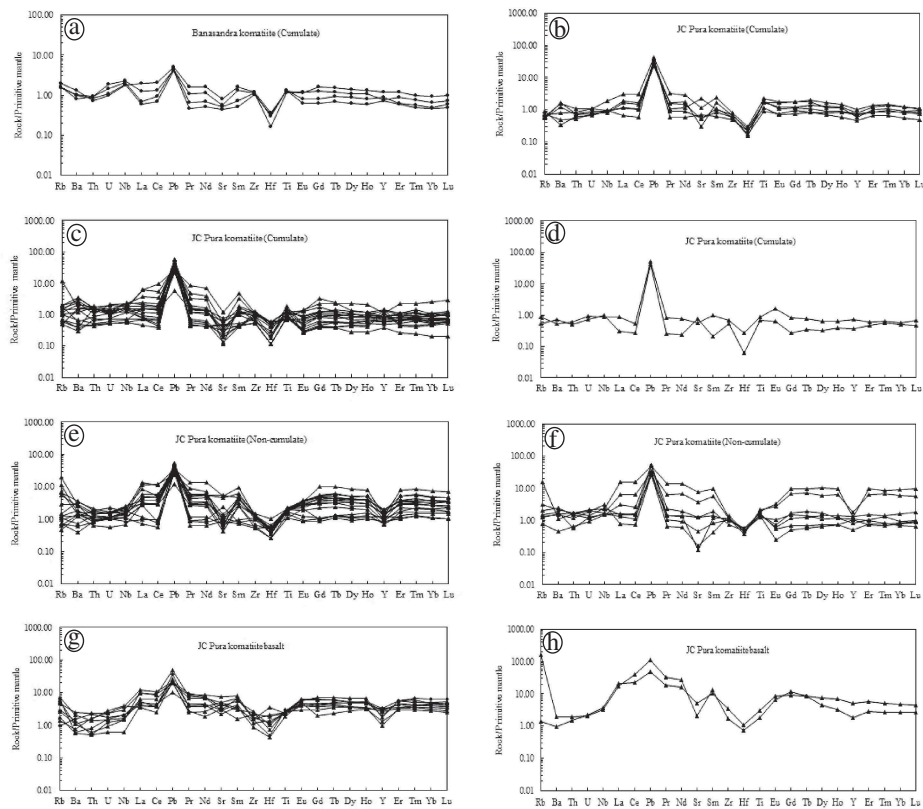


Figure 10. (a–h). Primitive mantle-normalized multi-element diagrams (Sun and McDonough 1989) of cumulate and non-cumulate komatiites from J.C. Pura, and Banasandra komatiite basalts of J.C. Pura greenstone belts.

In the Kunikenahalli–Kodihalli section of the Banasandra greenstone belt, the komatiite flows consist of flow units that constitute a compound flow field (Barnes 2006a) with a few massive undifferentiated flows, rare pillowed units, and sporadic komatiite hyaloclastite. Nearer to the vent, originally thin flows began to inflate and thicken, possibly into the undifferentiated massive flows. In thick sheet lobes, cooling produced rounded to elongated enclaves of massive komatiites that were previously interpreted as pillows (e.g. Figure 4 D-18 of Ramakrishnan and Vaidyanadhan 2008). Similar features are also reported from Munro township, where these are considered to have resulted from extremely curved cooling joints formed in massive komatiite flows (Arndt *et al.* 2008). Other examples include those described by Viljoen and Viljoen (1969), Arndt *et al.* (1977), Nisbet *et al.* (1977), and Imreh (1978), but many workers (e.g. Williams and Furnell 1979; Dann 2000) are not convinced that these structures formed as distinct entities, but are simply cells between large, curvilinear joints (Arndt *et al.* 2008).

In higher-effusion areas, flow front lobes rapidly extended the flow field. Pillows formed in areas of slope or low effusion. The rarity of pillows from the Kunikenahalli section may be due to the very low viscosity of high-Mg komatiites (Nisbet *et al.* 1977) and their

tendency to form compound flow lobes rather than pillowed flows. At the flow fronts or at break-outs near conduits, lava suffered quench fragmentation forming hyaloclastite. This could have occurred and been abundant at flow fronts and tops. Near the breakouts or near conduits, the fragments from the komatiite hyaloclastite mixed freely with the hot lava and produced the flowage of rafted clasts seen in some sections.

The lobes within the compound komatiite lava flow fields from Kunikenahalli are 1–5 m thick, similar to the dimensions of komatiite lobes from Munro township (Pyke *et al.* 1973; Shore 1996) and the Barberton greenstone belt (Smith *et al.* 1980; Viljoen *et al.* 1983). Thinner, undifferentiated flows, or A-zone-only flows, suggest marginal-lobate thin flows. The low viscosity of the komatiite lava was responsible for the development of a spinifex texture in liquids devoid of crystal nuclei; the spinifex developed only in the cooler, upper parts of the komatiite lobes from Kodihalli section as a result of large thermal gradients, coupled with heat transferred by radiation and convection within olivine crystals fixed in the cool upper layers of the lava flows (Shore and Fowler 1999).

Low-grade greenschist metamorphism led to the transformation of A-zone komatiites to chlorite schist, and corresponding stress deformed the spherical knobs to the augen-shaped structures seen in the lower part of the komatiite knobby flow exposed at the base of Rampura hill.

6.2. Widespread Palaeoarchaean komatiite volcanism and sub-contemporaneous TTG accretion in the western Dharwar craton

The time frame of volcanism in the older Sargur Group greenstone belts is not known precisely: detailed geochronological studies have not been initiated on lava flows of individual greenstone belts. Drury *et al.* (1987) obtained a Sm–Nd whole-isochron age of 2620 ± 55 Ma for mafic volcanics from the Holenarsipur greenstone belt, which is much younger compared with the ca. 3300 Ma SHRIMP U–Pb zircon age (Peucat *et al.* 1995) of felsic lava flows from higher stratigraphic levels of the same belt. Furthermore, detrital zircons from inter-layered sediments of the Holenarsipur belt indicate SHRIMP U–Pb ages ca. 3600–3200 Ma (Nutman *et al.* 1992; Bhaskar Rao *et al.* 2008). This discrepancy of a younger age obtained for Holenarsipur mafic-ultramafic rocks is not immediately clear, but could probably be related to resetting of the Sm–Nd system in response to intense fluid flow associated with metamorphism. Recently Jayananda *et al.* (2013b, 2015) have shown that fluid flow associated with 3.1 and 2.5 Ga metamorphic events caused alteration of initial Sr isotope ratios in TTGs, which is also in conformity with the Pb isotope study of Meen *et al.* (1992). On the other hand, Jayananda *et al.* (2008) dated Sargur Group komatiites from higher crustal levels affected by green schist metamorphism further northeast and presented a Sm–Nd whole-rock isochron age of 3352 ± 110 Ma. Among the individual greenstone belts, J.C. Pura komatiites define six sample Sm–Nd whole-rock isochron ages of 3384 ± 200 Ma corresponding to the oldest dated volcanism in the Dharwar craton (Jayananda *et al.* 2008). On the other hand, komatiites from the adjoining Kalyadi and Nuggihalli greenstone belts provided a less precise Sm–Nd whole-isochron age of 3284 ± 310 Ma (Jayananda *et al.* 2008). Furthermore, Maya *et al.* (2011) presented a Sm–Nd whole-rock isochron age of 3136 ± 200 Ma whilst Mondal *et al.* (2008) indicated 3156 ± 170 Ma for komatiites of the Nuggihalli belt. In summary, the published ages indicate a major episode of Palaeoarchaeon (ca. 3384–3250) komatiite volcanism with a minor pulse of Mesoarchaeon komatiite volcanism ca. 3150 Ma in the western Dharwar craton. These two episodes of komatiite volcanism are

sub-contemporaneous with two major TTG accretion events (ca. 3.4–3.3 and 3.23–3.15 Ga) in the western Dharwar cratons, as revealed by U–Pb zircon ages suggesting major events of crustal growth in the western Dharwar craton (Jayananda *et al.* 2015).

6.3. Effects of alteration

It is important to establish whether the chemistry of studied komatiites corresponds to their original composition or was affected by secondary processes. Globally elemental and isotope studies carried out on komatiites from major Archaean cratons reveal that the mobility of LILEs and other incompatible elements, including REEs, is controlled by fluid flow associated with metamorphism (Arndt *et al.* 1989; Tourpin *et al.* 1991; Gruau *et al.* 1992; Lahaye *et al.* 1995; Chavagnac 2004; Jayananda *et al.* 2008). On the other hand, Bau (1981) has shown that the mobility of REEs and other incompatible elements depends on their ability to form complexes with fluorine and/or CO₂-rich fluids. Furthermore, detailed isotopic (Nd–O–H–Ar) study of komatiites from the Schapenburg greenstone belt in southern Africa revealed that fluids did not disturb the REE patterns, except Eu (Lecuyer *et al.* 1994).

Recent elemental and Nd isotope studies on komatiites of the western Dharwar craton (Jayananda *et al.* 2008; Tushipokla and Jayananda 2013) have shown that REE and isotopic compositions were not significantly affected by post-magmatic fluid-induced alteration processes or metamorphism. The studied komatiites and komatiite basalts were affected by low-grade metamorphism and hydrothermal alteration, but volcanic structures and textures were well preserved. Primary mineralogy has been almost altered to secondary minerals such as serpentine, talc, tremolite, chlorite, and actinolite, except in rare instances where relicts of olivine are preserved. All the analysed samples from J.C. Pura and Banasandra show loss of ignition of <6 wt.%. However, petrographic evidence reveals the presence of carbonate, which occasionally forms microscopic networks of veins. Fluid-induced alteration, particularly carbonation, may have significantly affected certain major and trace element abundances, particularly LILEs (K, Rb, Ba, Sr), as reflected by scattering on Harker's binary diagrams (figures not shown) and crossing on primitive mantle-normalized multi-element diagrams (see Figure 10(a–h)). On the Nb/U *versus* Nb/Th plot, significant scattering (Figure 11(a)) indicates that U was affected by secondary processes. On the other hand, most analysed samples show uniform Al₂O₃/TiO₂ ratios, linear relations of Nb/Y *versus* the Zr/Y plot (Figure 11(b)), together with

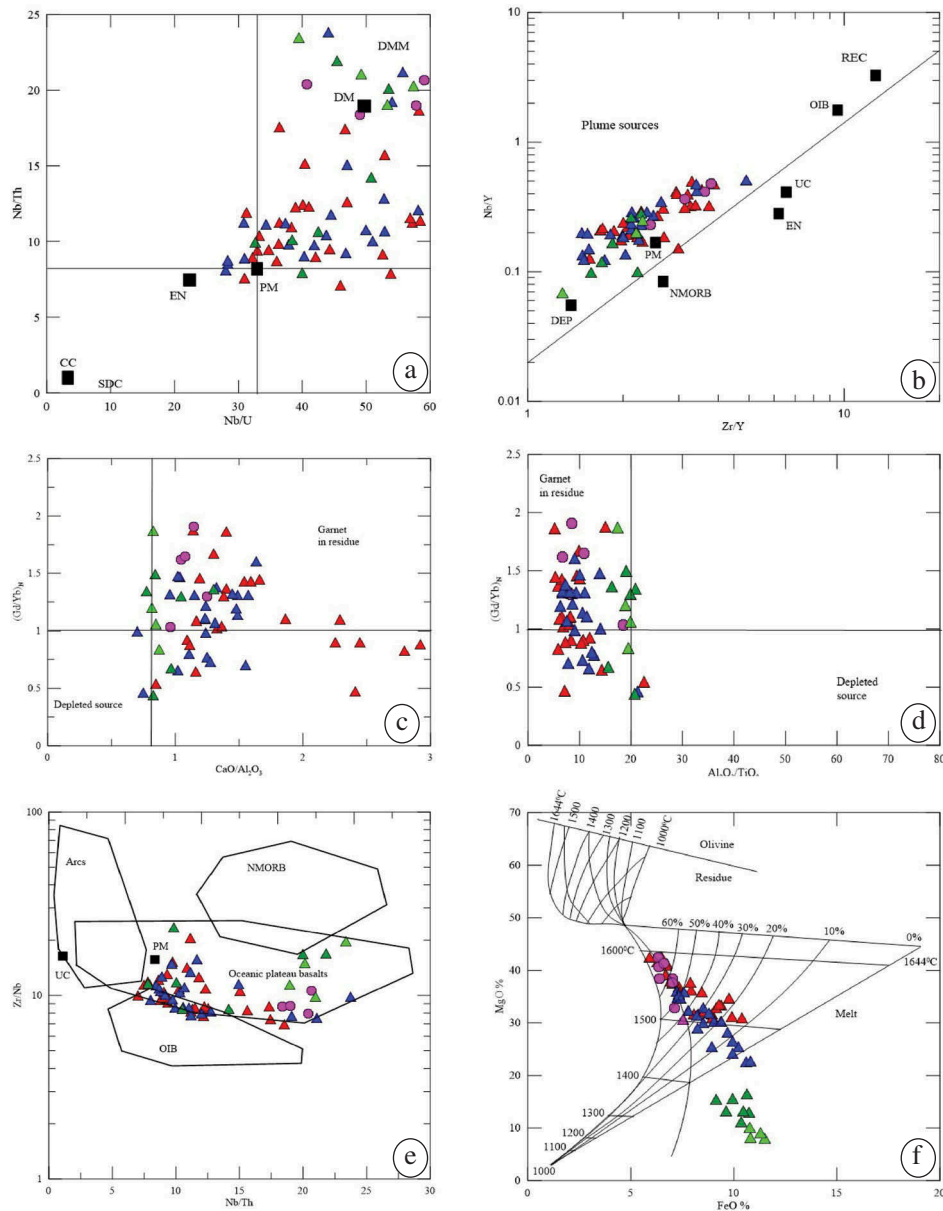


Figure 11. (a) Nb/U versus Nb/Th plot (after Saunders *et al.* 1988) showing scattering indicating source composition of primitive mantle to depleted MORB source mantle. (b) Nb/Y versus Zr/Y diagram (Condie 2003) showing dominant plume sources for the studied samples. (c) $(Gd/Yb)_N$ versus CaO/Al_2O_3 plot (after Jahn *et al.* 1982) showing role of residual garnet in the source for majority of studied samples. (d) $(Gd/Yb)_N$ versus Al_2O_3/TiO_2 (after Arndt 2003) indicating role of residual garnet for majority of komatiites. (e) Zr/Nb versus Nb/Th plot (Condie 2003) indicating the oceanic plateau basalt, with a few samples extending to ocean island basalt source. (f) MgO versus FeO plot (after Hanson and Langmuir 1978) showing komatiite melt equilibrium with mantle whilst komatiite basalts plot outside the liquidus field.

smooth REE patterns except for a few sample showing minor Ce and/or Eu anomalies, suggesting that alteration processes had no significant influence on REEs except Ce and Eu (see Figure 9(a–h)). On the contrary, the observed Ce and Eu anomalies may possibly be related to secondary processes. Among the samples showing Ce anomalies, the majority display negative anomalies except for three samples exhibiting positive anomalies. Several studies have convincingly shown

that Ce anomalies occur in response to oxidation of Ce^{+3} to Ce^{+4} and precipitation of Ce^{+4} as CeO_2 (e.g. Braun *et al.* 1993). The observed depletion of Ce and resulting negative anomalies can be attributed to removal of Ce by circulating fluid flow, whilst positive Ce anomalies are probably related to precipitation of Ce by fluid phase in an oxidizing environment. A few samples, despite their high MgO (30–42 wt.%) content, show either positive or negative Eu anomalies,

implying that most magnesium rocks were susceptible for alteration processes (c.f. Lecuyer *et al.* 1994; Fan and Kerrich 1997; Jayananda *et al.* 2008). Eu anomalies have also been attributed to seawater hydrothermal alteration, as suggested by Sun and Nesbitt (1978). The circulating fluid phase associated with hydrothermal plumbing systems probably resulted in the mobility of Eu. In summary, secondary processes did not affect the incompatible trace elements of studied komatiites except, to some extent, for LILE, U, Ce, and Eu contents. Consequently REEs and other immobile incompatible elements/elemental ratios are used in constraining mantle sources.

6.4. Crustal contamination

Geological, elemental, and isotopic compositions have been used to characterize contamination of komatiite magmas (Kerrich and Xie 2002). Field observations indicate that the studied komatiites formed in a marine environment and a far from sizeable older continental land mass. Published Nd isotope data [$\epsilon\text{Nd}(T) = 3.35 \text{ Ga} = +1.3$ to $+7.4$] do not indicate any contamination of much older continental crust (Jayananda *et al.* 2008). Furthermore, there are no trends of increasing SiO_2 or LREEs with increasing MgO, together with trace element characteristics – such as the absence of negative Nb–Ti anomalies on primitive mantle-normalized trace element diagrams – precluding any old crustal contamination. Komatiites with Nb/Th values <5 are considered to be contaminated with old crust (Condie 2003). However the higher Nb/Th (8–23) of the studied komatiites rules out any significant crustal contamination. Compared to primitive mantle, continental crust is characterized by a higher abundance of LREEs with depleted Nb, P, and Ti. In addition, continental crust shows a lower Ti/Zr ratio of 54 compared to the primitive mantle value of 116 (cf. Fan and Kerrich 1997). In the present study most Ti/Zr values of samples are high (>100), which precludes crustal contamination. These observations are further substantiated by La/Sm, Th/U, Zr/Nb, Nb/Y, and Zr/Y ratios of the majority of the samples being close to the recommended values of Archaean mantle (Campbell 2002; Condie 2003). Consequently the elemental and isotopic characteristics, in combination with the absence of any preserved continental crust older than 3.4 Ga, suggest that crustal contamination is not responsible for the observed elemental characteristics.

6.5. Petrogenesis and sources

Elemental and isotope studies of komatiites from Archaean cratons revealed their derivation from heterogeneous deep mantle sources (c.f. Arndt 2003).

However, the composition of mantle sources, the degree and depth of melting, and melting conditions varies globally over time.

6.5.1. Magmatic differentiation processes

Among the analysed samples of the J.C. Pura greenstone belt, 49 are komatiitic and 11 are komatiite basalt in composition. On the other hand, all six samples of the Banasandra belt are komatiite in composition. On the binary diagrams the studied komatiites and komatiite basalts together do not define linear trends for most of the major and trace elements, instead forming either two trends or komatiite basalts forming clusters. Such observed trends suggest that komatiites and komatiite basalts were not differentiated from single parental magma but evolved independently through melting of distinct mantle sources at different depths. The observed moderate to strong negative correlation of SiO_2 , Al_2O_3 , MnO, Fe_2O_3 , and CaO with MgO suggest the removal of olivine as a fractionated phase (see Figure 8) during differentiation of komatiite magma. This conclusion is supported by the strong positive correlation of Ni with MgO. The negative anomalies of Zr, Hf, and Y on primitive normalized spider diagrams indicate the role of garnet as a fractionating phase. On the other hand, the poorly defined trends or clustering of komatiite basalts on binary diagrams preclude a major fractionation process for the observed variation, although differentiation cannot be totally ruled out. In summary, the studied komatiites and komatiite basalt magmas are not related to differentiation of single parental magmas but evolved independently from parental magmas.

6.5.2. Nature and composition of mantle sources

In recent years elements/elemental ratios, together with worldwide isotope compositions of komatiites of different ages, have been used to constrain their mantle sources (Arndt *et al.* 2008). Al contents in komatiites have been used as an important criterion to characterize both the potential source and residual mineralogy of the mantle (Sun and Nesbitt 1978; Arndt 2003). Furthermore, based on Al contents, $(\text{Gd}/\text{Yb})_N$ ratios, and Ti, Y, Hf, and REEs, two type of komatiite have been identified: the Al-depleted Barberton type derived from deeper mantle with majorite garnet in the residue; and Al-non-depleted Munro type derived from melting of shallower mantle with no significant garnet in the residue (Arndt 2003). Both Al-depleted and -non-depleted komatiites correspond to essential melting of anhydrous mantle at different depths with varying residual mineralogy (Arndt *et al.* 2008). These conclusions are substantiated by experimental studies indicating

komatiite magma generation with or without the role of residual garnet (Ohtani *et al.* 1989; Herzberg 1999).

All studied komatiite samples of J.C. Pura show Al depletion, apart from three which show slightly lower CaO/Al₂O₃ (<1.0) despite lower Al₂O₃/TiO₂ (<18), whilst the komatiites of Banasandra show Al depletion. The three samples showing slightly lower CaO/Al₂O₃ despite their high MgO contents and lower Al₂O₃/TiO₂ are probably related to the mobility of CaO and its removal by a circulating CO₂-rich fluid phase during hydrothermal alteration processes deposited as tiny carbonate grains or microscopic veins (Chikhaoui 1981). This clearly indicates their derivation from deep mantle with the involvement of garnet in the source residue. On the other hand, low CaO/Al₂O₃ (<1.0) and high Al₂O₃/TiO₂ (>17, except for one sample at 15.9) values of J.C. Pura komatiite basalts imply their derivation from shallower mantle with no involvement of garnet in the residue. Major elements, in combination with (Gd/Yb)_N ratios, have been used to characterize the mantle and residual mineralogy of the source residue (Jahn *et al.* 1982). Most of the studied komatiites on bivariate plots of (Gd/Yb)_N versus CaO/Al₂O₃ (Figure 11(c)) and low Al₂O₃/TiO₂ (Figure 11(d)) indicate involvement of garnet in the residue, whilst fewer komatiite samples and the majority of komatiite basalts with lower (Gd/Yb)_N and sub-chondritic Al₂O₃/TiO₂ values imply the absence of significant garnet in the source residue. In Figure 11(d), the Al/Ti is non-chondritic-like ADK komatiites, but the (Gd/Yb)_N clusters around the chondrite line indicate Al/Ti fractionation but (Gd/Yb)_N do not show much fractionation. This is consistent with the flat REEs shown in Figure 9, precluding major garnet influence in the source. The majority of the studied komatiites show either chondritic (12.15–16.78 ppm) or sub-chondritic (2.31–4.92 ppm) total REEs, except for some samples with moderate to high total REEs (19.9–90.4 ppm) suggesting their derivation from heterogeneous sources ranging from highly depleted mantle to primitive mantle compositions. On the other hand, the wide range of REE contents of komatiitic basalts (21.66–150.37 ppm; see Figure 9(g, h)) also imply the involvement of heterogeneous sources and depleted to primitive mantle. Incompatible elements on primitive mantle-normalized diagrams are used to characterize mantle sources and residual mineralogy (Xie *et al.* 1993; McCuig *et al.* 1994; Fan and Kerrich 1997; Polat *et al.* 1999; Chavagnac 2004). Anomalies of Y, Hf, and Zr on multi-element diagrams have been used to constrain the nature of mantle sources and residual mineralogy (Fan and Kerrich 1997). The strong negative Hf, Zr, and Y anomalies on primitive mantle-normalized spider diagrams in the Al-depleted komatiites of Barberton, Dharwar, and

Superior Province have been attributed to komatiite magma generation at great depths with majorite garnet in the residue (Lahaye *et al.* 1995; Polat *et al.* 1999; Jayananda *et al.* 2008). Majorite garnet stability in mantle peridotite indicates pressures in the range 14–24 Gpa, corresponding to depths of magma generation below 400 km (Miller *et al.* 1991; Herzberg 1992; Xie *et al.* 1993; Fan and Kerrich 1997). Consequently, majorite retention in the residue results in strongly negative Hf, Zr, and Y anomalies. The majority of the Al-depleted J.C. Pura and Banasandra komatiites (see Figure 10(a–h)) display significant negative Hf, Zr, and Y anomalies, suggesting melt generation at deep mantle with the possible retention of majorite garnet in the residue. On the contrary, a few samples of Al-undepleted komatiites and komatiite basalts do show no significantly negative Hf, Zr, and Y, precluding the involvement of majorite garnet in the residue and reflecting melt segregation at shallower depths (~300–200 km). Nb anomalies on primitive mantle-normalized multi-element diagrams have been used to characterize mantle sources, particularly as a powerful fingerprint to discriminate between plume and arc sources (Jochum *et al.* 1991; Puchtel *et al.* 1997). Negative Nb anomalies have been interpreted in terms of either magma generation in very shallow mantle in arc environments or crustal contamination (Polat and Kerrich 2000), whereas positive Nb anomalies have been explained by melting of plume source in deep mantle or containing recycled slab component at great depths (Kerrich and Xie 2002). The majority of studied komatiites and komatiite basalts display either positive anomalies or no significant Nb anomalies, suggesting magma generation at great depth in hot-spot environments possibly associated with mantle plume. The presence of one komatiite and three komatiite basalts with slightly negative Nb anomalies could be related to melt generation in shallower mantle, or traces of contamination of recycled subduction-derived mafic arc crust.

Incompatible element ratios, such as Nb/Th and Nb/U, are considered to be useful in constraining the mantle sources of Archaean komatiites and basalts (Condie 2003). Figure 11(a) presents variation in Nb/Th and Nb/U where komatiites of J.C. Pura and Banasandra greenstone belts mainly plot in the fields defined for primitive mantle (PM) and depleted to deeply depleted mantle, whilst a few samples of komatiite basalts plot between PM and enriched mantle. The wider spread of the samples may be related to the mobility of U during secondary processes. Nb/Y and Zr/Y ratios can be used to distinguish different mantle sources of oceanic basalts and komatiites and can also provide important constraints on the tectonic setting, particularly in characterizing plume and N-MORB

settings (Fitton *et al.* 1997; Baksi 2001). Using Nb/Y and Zr/Y ratios Chavagnac (2004) has shown that Barberton komatiites are derived from a 'plume-like' mantle source and argue against subduction processes for the origin of komatiites. On the Nb/Y and Zr/Y diagram, all the studied west Dharwar komatiite samples plot on deep mantle plume sources, ranging in composition from primitive to depleted mantle (see Figure 11(b)). Average Zr/Nb and Nb/Th ratios of oceanic basalts and komatiites of different ages have been used for tracking mantle sources (Condie 2003). The majority of the komatiites and komatiite basalts in the present study plot in the oceanic plateau basalt field, with a few samples extending close to the OIB domain and corresponding to the PM source (Figure 11(e)). In summary, incompatible element ratios of komatiites and komatiite basalts reveal their derivation from heterogeneous deep mantle involving PM to depleted mantle source. This is in agreement with the published Nd isotope data of komatiites from the Dharwar craton indicating their derivation from heterogeneous mantle sources (Jayananda *et al.* 2008).

The majority of studies show that komatiites formed by a high degree of partial melting of hot ascending mantle plume (Arndt 2003). Elemental data, particularly Nb/Y and Zr/Y ratios, preclude the origin of the studied komatiites from shallow depleted mantle in MORB settings but suggest their derivation from a deep mantle plume source. However, the degree and depth of melting of the mantle are not known. The observed $\text{CaO}/\text{Al}_2\text{O}_3$ and $\text{Al}_2\text{O}_3/\text{TiO}_2$ values, $(\text{Gd}/\text{Yb})_N$ ratios, and negative anomalies of Zr, Hf, and Y on multi-element diagrams suggest the generation of komatiite magmas at great depth (ca. 400 km), whilst komatiite basalts were probably generated at relatively shallower depths (ca. 250–300 km). The MgO-FeO diagram of Hanson and Langmuir (1978) has been used to assess liquidus temperatures, as well as the degree of melting and to evaluate the relationship between peridotitic komatiites and komatiite basalts. The MgO-FeO data of studied komatiites and komatiite basalts projected on the diagram (Figure 11(f)) show that only komatiites plotting in the liquidus field could have co-existed in equilibrium with peridotitic upper mantle. On the other hand, komatiite basalts plot outside the liquidus field (see Figure 11(f)), indicating that melts were not in equilibrium with peridotitic mantle and were probably generated in shallow mantle and emplaced before acquiring an ultramafic composition. The komatiite melts were probably generated by high-degree melting (20–60%) with initial melt temperatures as high as 1450–1550°C, whilst komatiite basalts were formed by low-degree melting (10–20%) with initial

temperatures of 1300–1400°C. Thus it is more likely that komatiites and komatiite basalt magmas were generated at different depths in mantle by varying degrees of partial melting.

6.6. Implications for the Archaean mantle

Nd and Hf isotope data show that Eoarchaeon ultramafic/mafic rocks formed from mantle reservoir are already depleted in incompatible elements (Bennett *et al.* 1993; Blichert-Toft and Arndt 1999; Hoffmann *et al.* 2011; Nebel *et al.* 2014). Increasing Nd and Hf isotope evidence is also presented for Palaeoarchaeon komatiites (ϵNd values ranging +2 to +5 at 3.4 Ga) from different cratons (Chavagnac 2004; Jayananda *et al.* 2008). The two element pairs Nb/U and Th/U are useful to characterize the long-term evolution of depleted mantle reservoirs and complementary growth of continental crust. The Nb/U and Th/U ratios of PM we found to be 34 and 4.04, respectively (Sun and McDonough 1989).

Campbell (2002) has shown that extraction of continental crust alters the Nb/U ratio of the mantle without affecting the Nb/Th ratio, whilst extraction of mid-ocean ridge basalt resulted in altered Th/U with no effect on Nb/U. Such changes in ratios of incompatible elements can be used to characterize mantle evolution during extraction of oceanic crust and continental crust. On the Nb/Th versus Nb/U plot (see Figure 11(a)), the studied rocks show a wide range of PM through depleted mantle to deeply depleted mantle, suggesting large-scale heterogeneity of Archaean mantle and, in particular, the existence of highly depleted mantle reservoirs during the Palaeoarchaeon. A highly depleted mantle signature is also revealed by sub-chondritic REE contents in a significant number of komatiite samples (see Figure 9(a–h)), which in turn is substantiated by Nd isotope data [$\epsilon\text{Nd}(T) = 1.3$ to 7.4] for west Dharwar komatiites (Jayananda *et al.* 2008; Jayananda, unpublished data). The existence of such highly depleted deep mantle reservoirs implies differentiation of mantle in an earlier crust-forming event, possibly in the form of oceanic plateaus. Elemental and Nd-Pb isotope data of Palaeoarchaeon (3.4–3.3 Ga) felsic crust (TTG-gneisses) in western Dharwar craton suggest their derivation from shallow depleted mantle, possibly in arc environments (Meen *et al.* 1992; Peucat *et al.* 1993; Naqvi *et al.* 2009; Jayananda *et al.* 2015). Consequently, elemental and isotope data of the Palaeoarchaeon komatiites and TTG show depletion of both deep and shallow mantle reservoirs. Such depletion of Palaeoarchaeon mantle reservoirs implies an earlier episode of crustal growth, probably during the

Eoarchaeon. Although the precise ages of Eoarchaeon (ca. 3.8 Ga) crustal record have not been documented for the Dharwar craton, Nd model ages (Jayananda *et al.* 2015) and a single zircon grain age of ca. 4.0 Ga (Santosh *et al.* 2015) suggest remnants of Eoarchaeon–Headen crust. Alternatively, such highly depleted mantle reservoirs were attributed to early global differentiation of silicate earth by Boyet and Carlson (2005). More recent studies also document the existence of terrestrial crust as old as 4.37 Ga (Holden *et al.* 2009; Iizuka *et al.* 2011; Roth *et al.* 2013). Consequently the above arguments suggest that the Palaeoarchaeon mantle was highly heterogeneous but generally variably depleted. Such long-term depletion of mantle reservoirs is probably related to either an earlier episode of Eoarchaeon crust accretion or global differentiation of silicate earth. More detailed elemental data, in combination with ^{142}Nd and ^{143}Nd data, are needed to address these issues.

6.7. Tectonic context of magma generation and eruption

Globally two principal end member models involving plume or horizontal tectonics have been proposed to explain komatiite magma generation and the eruption of komatiite. Most workers proposed a mantle plume model (Ohtani *et al.* 1989; Arndt 2003) where komatiite erupted in either a plume-related intraplate environment (Lahaye *et al.* 1995; Herzberg 1999) or plume-derived oceanic plateaus (Condie and Abbott 1999; Kerr *et al.* 2000; Polat and Kerrich 2000; Chavagnac 2004; Jayananda *et al.* 2008). However, Parman *et al.* (2001) and Grove *et al.* (1999) proposed the generation and emplacement of Barberton komatiite magmas in an arc setting whilst De Wit *et al.* (1987) attributed komatiite magma generation and eruption in the divergent setting of an oceanic spreading centre.

Field observations provide first-order constraints on the tectonic context of komatiite eruption. The observed spectacular pillows/pillow breccias/flow top breccias (see Figure 5(g–h)) in the J.C. Pura and Banasandra greenstone belts indicate a marine environment of eruption, which precludes the eruption of the studied komatiites in the context of continental flood basalt settings. The close association of pillows and adjoining areas with spinifex structures implies a shallow marine environment with small volcanic islands/oceanic plateaus. The presence of interlayered quartzite/chert also suggests shallow marine environment.

Elemental and isotopic data provide important constraints on the tectonic context of magma generation. Magmas generated in subduction-related arc settings

show distinct elemental characteristics compared to those generated in hot-spot environments associated with mantle plume. Contents of elements such as Nb, Ta, Hf, Zr, Y, and Ti, and ratios such as Nb/Th, Nb/U, Nb/Y, and Zr/Y, can be used to discriminate between arc and plume settings (Campbell 2002; Condie 2003). Magmas generated in arc settings show characteristic depletion of Nb, Ta, and Ti and enrichment in Th, U, Ba, Rb, and Sr, whilst magmas generated in plume settings show no depletion of Nb, Ta, and Ti but display strong depletion of Hf, Zr, and Y. However, Parman *et al.* (2001) have argued that Barberton komatiites can be generated in subduction zone environments. The geochemical characteristics of the studied komatiites and komatiite basalts such as $\text{CaO}/\text{Al}_2\text{O}_3$, $\text{Al}_2\text{O}_3/\text{TiO}_2$ ratios with positive or no Nb anomalies, in combination with strongly negative Zr, Hf, and Y anomalies on multi-element diagrams (see Figure 10(a–h)), preclude their derivation from mantle source but are consistent with their generation in deep mantle hot-spot environments similar to modern mantle plume. This argument can be further substantiated by Nb/Y versus Zr/Y (see Figure 11(b)) and Zr/Nb versus Nb/Th plots (see Figure 11(e)), which suggest the generation of komatiite magmas in a plume setting. To summarize, petrologic and elemental data show that komatiites were generated in deep mantle in association with rising mantle plume and erupted in marine environments (Figure 12(a, b)).

7. Conclusions

The conclusions of the study can be summarized as follows.

- (1) Widespread komatiite–komatiite basalt magmatism occurred in the western Dharwar craton 3.38–3.2 Ga, which is sub-contemporaneous with adjoining TTG accretion.
- (2) Pillow breccias, hyaloclastites, and spinifex structure together with elemental data suggest very high eruption temperatures (~1450–1550°C).
- (3) Incompatible element data of the studied komatiites show their derivation from heterogeneous sources ranging in composition from highly depleted to primitive mantle.
- (4) The existence of deep depleted mantle 3.38–3.2 Ga imply large-scale mantle differentiation and crustal growth, probably ca. 3.6–3.8 Ga.
- (5) Elemental data suggest the derivation of komatiite magma in hot-spot environments associated with rising mantle plume.

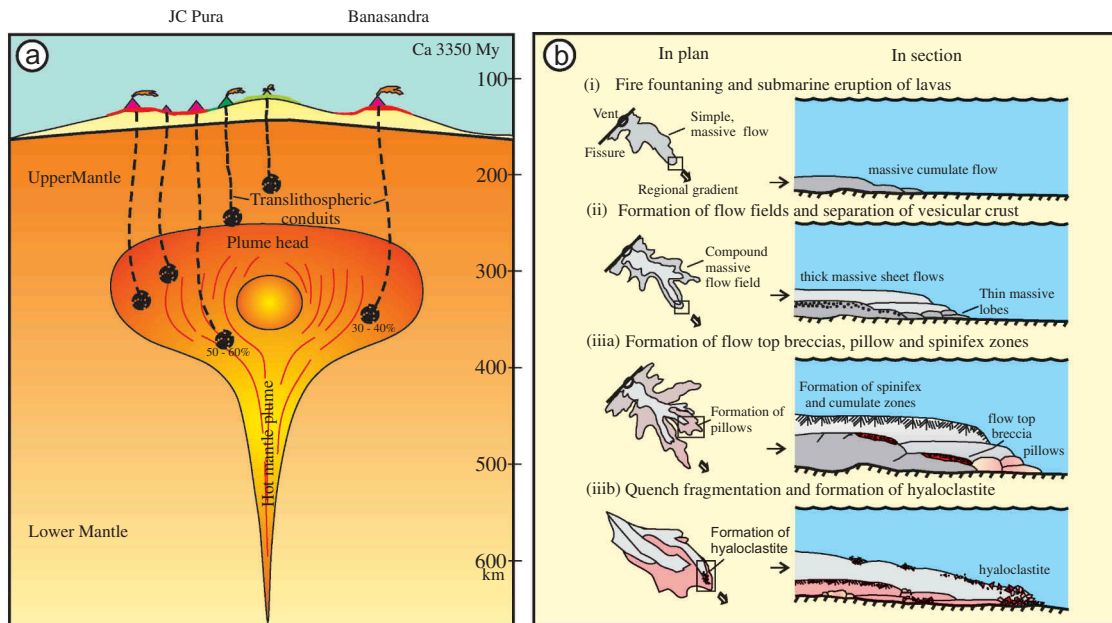


Figure 12. (a) Cartoon depicting plume model for the generation of studied komatiites and komatiite basalts. Percentages indicate degree of partial melting. (b) Emplacement mechanism of komatiite lava flows.

Acknowledgements

This work was financially supported by DST-funded project (ESS/16/334/2007/dated 14-10-2008) and continued by U.G.C project (42/72/2013(SR)). The Director, Dr V. Balaram and Dr M. Satyanarayanan of the National Geophysical Research Institute (NGRI), Hyderabad are thanked for providing ICP-MS facilities for trace element analysis. We are extremely thankful to David Mole for stimulating reviews and R.J. Stern for editorial guidance that substantially enhanced the quality of this contribution.

Disclosure statement

No potential conflict of interest was reported by the authors.

Funding

This work was financially supported by DST-funded project [ESS/16/334/2007] dated 14-10-2008 and continued by U.G.C project [42/72/2013(SR)].

ORCID

Tushipokla  <http://orcid.org/0000-0001-8373-9174>

References

Anand, R., and Balakrishnan, S., 2010, Pb, Sr and Nd isotope systematics of metavolcanic rocks of the Hutti greenstone belt, Eastern Dharwar craton: Constraints on age, duration of volcanism and evolution of mantle sources during late

- Archean: *Journal of Asian Earth Sciences*, v. 39, p. 1–11. doi:10.1016/j.jseaes.2010.02.010
- Arndt, N., 2003, Komatiites, kimberlites and boninites: *Journal of Geophysical Research*, v. 108, p. 2293–2304. doi:10.1029/2002JB002157
- Arndt, N., Leshner, C.M., Houlié, M.G., Lewin, E., and Lacaze, Y., 2004, Intrusion and crystallization of a spinifex-textured komatiite sill in Dundonald Township, Ontario: *Journal of Petrology*, v. 45, p. 2555–2571.
- Arndt, N.T., 1994, Archean komatiites, in Condie, K.C., ed., *Archean crustal evolution: Amsterdam, Elsevier*, 11–44 p.
- Arndt, N.T., Leshner, C.M., and Barnes, S.J., 2008, *Komatiites: New York, Cambridge University Press*, 467 p.
- Arndt, N.T., Naldrett, A.J., and Pyke, D.R., 1977, Komatiitic and Fe-rich tholeiitic lavas of Munro Township, northeastern Ontario: *Journal of Petrology*, v. 18, p. 319–369. doi:10.1093/petrology/18.2.319
- Arndt, N.T., and Nisbet, E.G., 1982, *Komatiites: UK, George Allen and Unwin Publications*, 526 p.
- Arndt, N.T., Teixeira, N.A., and White, W.M., 1989, Bizarre geochemistry of komatiites from the Crixas greenstone belt, Brazil: *Contributions to Mineralogy and Petrology*, v. 101, p. 187–197. doi:10.1007/BF00375305
- Baksi, A.K., 2001, Search for a deep mantle component in mafic lava using a Nb-Y-Zr plot: *Canadian Journal of Earth Sciences*, v. 38, p. 813–824.
- Balakrishnan, S., Hanson, G.N., and Rajamani, V., 1990, Pb and Nd isotope constraints on the origin of high Mg and tholeiitic amphibolites, Kolar Schist belt, South India: *Contributions to Mineralogy and Petrology*, v. 107, p. 272–292.
- Balakrishnan, S., and Rajamani, V., 1987, Geochemistry and petrogenesis of granitoids around the Kolar Schist Belt, south India: Constraints for the evolution of the crust in the Kolar area: *The Journal of Geology*, v. 95, p. 219–240. doi:10.1086/629121

- Balakrishnan, S., Rajamani, V., and Hanson, G.N., 1999, U–Pb ages for zircon and titanite from the Ramagiri area, southern India: Evidence for accretionary origin of the eastern Dharwar craton during the late Archaean: *Journal of Geology*, v. 107, p. 69–86. doi:10.1086/314331
- Balaram, V., and Gnanaswar Rao, T., 2003, Rapid determination of REE and other trace elements in geological samples by microwave acid digestion and ICP-MS: *Atomic Spectroscopy*, v. 24, p. 206–212.
- Barnes, S.J., 2006a, Komatiite-hosted nickel sulfide deposits: Geology, geochemistry, and genesis: Society of Economic Geologists Special Publication, v. 13, p. 51–118.
- Barnes, S.J., 2006b, Komatiites: Petrology, volcanology, metamorphism and geochemistry: Society of Economic Geologists Special Publication, v. 13, p. 13–49.
- Barnes, S.J., Hill, R.E.T., and Gole, M.J., 1988, The perseverance ultramafic complex, Western Australia: The product of a komatiite lava river: *Journal of Petrology*, v. 29, p. 305–331. doi:10.1093/petrology/29.2.305
- Bau, M., 1981, Rare earth mobility during hydrothermal and metamorphic fluid-rock interaction and the significance of the oxidation state of europium: *Chemical Geology*, v. 93, p. 219–230. doi:10.1016/0009-2541(91)90115-8
- Bennett, V.C., Nutman, A.P., and McCulloch, M.T., 1993, Nd isotopic evidence for transient, highly depleted mantle reservoirs in the early history of the Earth: *Earth and Planetary Science Letters*, v. 119, p. 299–317. doi:10.1016/0012-821X(93)90140-5
- Beresford, S.W., Cas, R.A.F., Lambert, D.D., and Stone, W.E., 2000, Vesicles in thick komatiite lava flows, Kambalda, Western Australia: *Journal of the Geological Society*, v. 157, p. 11–14. doi:10.1144/jgs.157.1.11
- Bhaskar Rao, Y.J., Griffin, W.L., Ketchum, J., Pearson, N.J., Beyer, E., and O'Reilly, S.Y., 2008, An outline of juvenile crust formation and recycling history in the archaean western dharwar craton, from zircon in situ U-Pb dating and Hf-isotopic compositions. abstract, goldschmidt conference 2008: *Geochimicaet Cosmochimica Acta*, v. 72, p. A81.
- Bhaskar Rao, Y.J., Sivaraman, T.V., Pantulu, C.V.C., Gopalan, K., and Naqvi, S.M., 1992, Ages of late Archaean metavolcanics and granites, Dharwar craton: Evidence for early Proterozoic thermo-tectonic events: *Precambrian Research*, v. 38, p. 246–270.
- Bidyananda, M., Goswami, J.N., and Srinivasan, R., 2011, Pb–Pb zircon ages of Archean meta- sediments and gneisses from the Dharwar Craton, southern India: Implications for the antiquity of the eastern dharwar craton: *Journal of Earth System Science*, v. 120, p. 643–661. doi:10.1007/s12040-011-0094-1
- Blichert-Toft, J., and Arndt, N.T., 1999, Hf isotope compositions of komatiites: *Earth and Planetary Science Letters*, v. 171, no. 3, p. 439–451. doi:10.1016/S0012-821X(99)00151-X
- Bouhallier, H., Chardon, D., and Choukroune, P., 1995, Strain patterns in Archaean dome-and-basin structures: The Dharwar craton (Karnataka, south India): *Earth and Planetary Science Letters*, v. 135, p. 57–75. doi:10.1016/0012-821X(95)00144-2
- Boyet, M., and Carlson, R.W., 2005, ¹⁴²Nd evidence for early (>4.53 Ga) global differentiation of silicate Earth: *Science*, v. 309, p. 577–581. doi:10.1126/science.1113634
- Braun, J.J., Pagel, M., Herbillon, A., and Rosin, C., 1993, Mobilization and redistribution of REEs and thorium in a syenitic lateritic profile: A mass balance study: *Geochimicaet Cosmochimica Acta*, v. 57, p. 4419–4434. doi:10.1016/0016-7037(93)90492-F
- Campbell, I.H., 2002, Implications of Nb/U, Th/U and Sm/Nd in plume magmas for the relationship between continental and oceanic crust formation and the development of the depleted mantle: *Geochimicaet Cosmochimica Acta*, v. 66, p. 1651–1661. doi:10.1016/S0016-7037(01)00856-0
- Chadwick, B., Vasudev, V.N., and Hedge, G.V., 2000, The Dharwar craton, southern India, interpreted as the result of late Archaean oblique convergence: *Precambrian Research*, v. 99, p. 91–101. doi:10.1016/S0301-9268(99)00055-8
- Chadwick, B., Vasudev, V.N., Hegde, G.V., and Nutman, A.P., 2007, Structure and SHRIMP U/Pb zircon ages of granites adjacent to the chitradurga schist belt: Implications for Neoproterozoic convergence in the Dharwar craton, southern India: *Journal of the Geological Society of India*, v. 69, p. 5–24.
- Charan, S.N., Naqvi, S.M., and Ramesh, S.L., 1988, Geology and geochemistry of spinifex textured peridotitic komatiite from Mayasandra Schist Belt: *Journal of the Geological Society of India*, v. 32, p. 343–350.
- Chardon, D., Choukroune, P., and Jayananda, M., 1996, Strain patterns, décollement and incipient sagducted greenstone terrains in the Archaean Dharwar craton (South India): *Journal of Structural Geology*, v. 18, p. 991–1004. doi:10.1016/0191-8141(96)00031-4
- Chardon, D., and Jayananda, M., 2008, Three dimensional field perspective on deformation, flow, and growth of the lower continental crust (Dharwar craton, India): *Tectonics*, v. 27, p. TC1014. doi:10.1029/2007TC002120
- Chardon, D., Jayananda, M., Chetty, T.R.K., and Peucat, -J.-J., 2008, Precambrian continental strain and shear zone patterns: The South Indian case: *Journal of Geophysical Research*, v. 113, no. B08402. doi:10.1029/2007JB005299
- Chardon, D., Jayananda, M., and Peucat, -J.-J., 2011, Lateral constriction flow of hot orogenic crust: Insights from the Neoproterozoic of south India, geological and geophysical implications for orogenic plateaux: *Geochimicaet Cosmochimica Acta*, v. 75, p. Q02005. doi:10.1029/2010GC003398
- Chardon, D., Peucat, -J.-J., Jayananda, M., Choukroune, P., and Fanning, C.M., 2002, Archaean granite-greenstone tectonics at Kolar (South India): Interplay of diapirism and bulk inhomogeneous contraction during magmatic juvenile accretion: *Tectonics*, v. 21. doi:10.1016.1029/2001TC901032
- Chavagnac, V., 2004, A geochemical and Nd isotopic study of Barberton komatiites (South Africa): Implication for the Archean mantle: *Lithos*, v. 75, p. 253–281. doi:10.1016/j.lithos.2004.03.001
- Chikhaoui, M., 1981, Les roches volcaniques du proterozoique-superieur de la chaine pan-Africaine dans le NW de l' Afrique (Hoggar, Anti-Atlas, Adirades Iforas): *Caracterisation geochimique et mineralogique, implications geodynamiques.* Montpellier, These d' Etat, 183 p.
- Condie, K.C., 2003, Incompatible element ratios in oceanic basalts and komatiites: Tracking deep mantle sources and continental growth rates with time: *Geochimicaet Cosmochimica Acta*, v. 67, p. 1–28. doi:10.1029/2002GC000333
- Condie, K.C., and Abbott, D.H., 1999, Oceanic plateaus and hotspot islands: Identification and role in continental growth: *Lithos*, v. 46, p. 1–4.

- Dann, J.C., 2000, The 3.5 Ga komati formation, barberton greenstone belt, South Africa. Part I: New maps and magmatic architecture. *South African Journal of Geology*, v. 103, no. 1, p. 47–68.
- Dann, J.C., 2001, Vesicular komatiites, 3.5-Ga Komati formation, barberton greenstone belt, South Africa: Inflation of submarine lavas and origin of spinifex zones: *Bulletin of Volcanology*, v. 63, p. 462–481. doi:10.1007/s004450100164
- De Wit, M.J., Hart, R.A., and Hart, R.J., 1987, The Jamestown ophiolite complex, Barberton mountain belt: A section through 3.5 Ga oceanic crust: *Journal of African Earth Sciences*, v. 6, p. 681–730. doi:10.1016/0899-5362(87)90007-8
- Devapriyan, G.V., Anantharamu, T.R., Vidyadharan, K.T., and Raghu Nandan, K.R., 1994, Spinifex textured peridotitic komatiite from Honnabetta area, Nagamangala schist belt, Karnataka: *Journal of Geological Society of India*, v. 44, p. 483–493.
- Dey, S., 2013, Evolution of Archean crust in the Dharwar craton: The Nd isotope record: *Precambrian Research*, v. 227, p. 227–246. doi:10.1016/j.precamres.2012.05.005
- Dostal, J., and Mueller, W.U., 2012, Deciphering an Archean mantle plume: Abitibi Greenstone Belt, Canada: *Gondwana Research*, v. 23, p. 493–505. doi:10.1016/j.gr.2012.02.005
- Drury, S.A., Van Calstren, P.C., and Reeves-Smith, G.J., 1987, Sm–Nd isotopic data from Archaean metavolcanic rocks at Holenarasipur, South India: *Journal of Geology*, v. 95, p. 837–843. doi:10.1086/629182
- Duraiswami, R.A., Inamdar, M.M., and Shaikh, T.N., 2013, Emplacement of pillow lavas from the ~ 2.8 Ga Chitradurga Greenstone Belt, South India: A physical volcanological, morphometric and geochemical perspective: *Journal of Volcanology and Geothermal Research*, v. 264, p. 134–149. doi:10.1016/j.jvolgeores.2013.08.002
- Fan, J., and Kerrich, R., 1997, Geochemical characteristics of Al-depleted and undepleted komatiites and HREE-enriched tholeiites, western Abitibi greenstone belt: Variable HFSE/REE systematics in a heterogeneous mantle plume: *Geochimica et Cosmochimica Acta*, v. 61, p. 4723–4744. doi:10.1016/S0016-7037(97)00269-X
- Fitton, J.G., Saunders, A.D., Norry, M.J., Hardarson, B.S., and Taylor, R.N., 1997, Thermal and chemical structure of the Iceland plume: *Earth and Planetary Science Letters*, v. 153, p. 197–208. doi:10.1016/S0012-821X(97)00170-2
- Furnes, H., De Wit, M., and Robins, B., 2013, A review of new interpretations of the tectonostratigraphy, geochemistry and evolution of the onverwacht suite, barberton greenstone belt, South Africa: *Gondwana Research*, v. 23, p. 403–428. doi:10.1016/j.gr.2012.05.007
- Grove, T.L., Dewit, M.J., and Dann, J., 1997, in Dewit, M.J., and Ashwal, L.D., eds., Komatiites from the Komati type section, Barberton, South Africa, in Dewit, M.J., and Ashwal, L.D., eds., *Greenstone belts*: Oxford, Oxford University Press, p. 422–437.
- Grove, T.L., Parman, S.W., and Dann, J.C., 1999, Conditions of magma generation for Archaean komatiites from the Barberton Mountain land, South Africa, in Fei, Y., Bertka, C. M., and Mysen, B.O., eds., *Mantle petrology: Field observations and high pressure experimentation*: Lancaster, The Geochemical Society, Cadmus Journal Services, 155–167 p.
- Gruau, G., Toupin, S., Fourcade, S., and Blais, S., 1992, Loss of isotopic (Nd, O) and chemical (REE) memory during metamorphism of komatiites: New evidence from eastern Finland: *Contribution to Mineralogy and Petrology*, v. 112, p. 66–82. doi:10.1007/BF00310956
- Hanson, G.N., and Langmuir, C.H., 1978, Modelling of major elements in mantle melt systems using trace element approaches: *Geochimica et Cosmochimica Acta*, v. 42, p. 725–741. doi:10.1016/0016-7037(78)90090-X
- Herzberg, C., 1992, Depth and degree of melting of komatiites: *Journal of Geophysical Research*, v. 97, p. 4521–4540. doi:10.1029/91JB03066
- Herzberg, C., 1995, Generation of plume magmas through time - an experimental perspective: *Chemical Geology*, v. 126, p. 1–16. doi:10.1016/0009-2541(95)00099-4
- Herzberg, C., 1999, Phase equilibrium constraints on the formation of cratonic mantle, in Fei, Y., Bertka, C.M., and Mysen, B.O., eds., *Mantle petrology: Field observations and high-pressure experimentation*, vol. 6. Special Publication: Geochemical Society, p. 241–257.
- Herzberg, C., and O'Hara, M.J., 1998, Phase equilibrium constraints on the origin of basalts, picrites, and komatiites: *Earth Science Review*, v. 44, p. 39–79. doi:10.1016/S0012-8252(98)00021-X
- Hill, R.E.T., Barner, S.J., Gole, M.J., and Dowling, S.E., 1995, The volcanology of komatiites as deduced from field relationships in the Norman-Wiluna Greenstone Belt, Western Australia: *Lithos*, v. 34, p. 159–188. doi:10.1016/0024-4937(95)90019-5
- Hoffmann, J.E., Münker, C., Polat, A., Rosing, M.T., and Schulz, T., 2011, The origin of decoupled Hf–Nd isotope compositions in Eoarchean rocks from southern West Greenland: *Geochimica et Cosmochimica Acta*, v. 75, no. 21, p. 6610–6628. doi:10.1016/j.gca.2011.08.018
- Holden, P., Lanc, P., Ireland, T.R., Harrison, T.M., Foster, J.J., and Bruce, Z., 2009, Mass-spectrometric mining of Hadean zircons by automated SHRIMP multi-collector and single-collector U/Pb zircon age dating: The first 100,000 grains: *International Journal of Mass Spectrometry*, v. 286, p. 53–63. doi:10.1016/j.ijms.2009.06.007
- Huppert, H.E., and Sparks, R.S.J., 1985, Komatiites I; eruption and flow: *Journal of Petrology*, v. 26, p. 694–725. doi:10.1093/petrology/26.3.694
- Iizuka, T., Nebel, O., and McCulloch, M.T., 2011, Tracing the provenance and recrystallization processes of the Earth's oldest detritus at Mt. Narryer and Jack Hills, Western Australia: An in situ Sm–Nd isotopic study of monazite: *Earth Planetary Science Letters*, v. 308, no. 3–4, p. 350–358. doi:10.1016/j.epsl.2011.06.006
- Imreh, L., 1978, Album photographique de coulées métavolcaniques sous-marines archéennes dans le sillon de La Motte-Vassan [Photographic Album of Submarine Archaean Meta-Ultramafic Flows in the LaMotte–Vassan Belt]: Quebec, Ministère des Richesses Naturelles.
- Jahn, B.M., Auvray, B., Blais, S., Capdevila, R., Cornichet, J., Vidal, F., and Hameurt, J., 1980, Trace element geochemistry and petrogenesis of Finnish greenstone belts: *Journal of Petrology*, v. 21, no. 2, p. 201–244. doi:10.1093/petrology/21.2.201
- Jahn, B.-M., Gruau, G., and Glikson, A.Y., 1982, Komatiites of the Onverwacht Group, S. Africa: REE geochemistry, Sm/Nd age, and mantle evolution: *Contributions to Mineralogy and Petrology*, v. 80, p. 25–40. doi:10.1007/BF00376732
- Jayananda, M., Banerjee, M., Pant, N.C., Dasgupta, S., Kano, T., Mahesha, N., and Mahableswar, B., 2011, 2.62 Ga high-

- temperature metamorphism in the central part of the eastern Dharwar craton: Implications for late Archaean tectono-thermal history: *Geological Journal*, v. 46. doi:10.1002/gj.1308
- Jayananda, M., Chardon, D., Peucat, J.J., and Capdevila, R., 2006, 2.61 Ga potassic granites and crustal reworking in the Western Dharwar Craton (India): Tectonic, geochronologic and geochemical constraints: *Precambrian Research*, v. 150, p. 1–26. doi:10.1016/j.precamres.2006.05.004
- Jayananda, M., Chardon, D., Peucat, J.-J., and Fanning, C.M., 2015, Paleo- to Mesoproterozoic TTG accretion and continental growth, western Dharwar craton, southern India: SHRIMP U-Pb zircon geochronology, whole-rock geochemistry and Nd-Sr isotopes: *Precambrian Research*, v. 268, p. 295–322. doi:10.1016/j.precamres.2015.07.015
- Jayananda, M., Kano, T., Peucat, J.-J., and Channabasappa, S., 2008, 3.35 Ga komatiite volcanism in the western Dharwar craton, southern India: Constraints from Nd isotopes and whole-rock geochemistry: *Precambrian Research*, v. 162, p. 160–179. doi:10.1016/j.precamres.2007.07.010
- Jayananda, M., Martin, H., Peucat, J.-J., and Mahabaleswar, B., 1995, Late Archaean crust-mantle interactions: Geochemistry of LREE-enriched mantle derived magmas. Example of the Closepet batholith, Southern India: *Contribution to Mineralogy Petrology*, v. 119, p. 314–329. doi:10.1007/BF00307290
- Jayananda, M., Moyen, J.-F., Martin, H., Peucat, J.-J., Auvray, B., and Mahabaleswar, B., 2000, Late Archaean (2550–2520 Ma) juvenile magmatism in the Eastern Dharwar Craton, southern India: Constraints from geochronology, Nd-Sr isotopes and whole rock geochemistry: *Precambrian Research*, v. 99, p. 225–254. doi:10.1016/S0301-9268(99)00063-7
- Jayananda, M., Peucat, J.-J., Chardon, D., Krishnarao, B., and Corfu, F., 2013a, Neoproterozoic greenstone volcanism, Dharwar craton, southern India: Constraints from SIMS zircon geochronology and Nd isotopes: *Precambrian Research*, v. 227, p. 55–76. doi:10.1016/j.precamres.2012.05.002
- Jayananda, M., Tsutsumi, Y., Miyazaki, T., Gireesh, R.V., Kapfo, K.-U., Tushipokla, H., and Kano, T., 2013b, Geochronological constraints on Meso- and Neoproterozoic regional metamorphism and magmatism in the Dharwar craton, southern India: *Journal of Asian Earth Sciences*. doi:10.1016/j.jseaes.2013.04.033.
- Jenner, G.A., Longerich, H.P., Jackson, S.E., and Fryer, B.J., 1990, ICP-MS – a powerful tool for high precision trace element analysis in earth sciences: Evidence from analysis of selected USGS reference samples: *Chemical Geology*, v. 83, p. 133–148. doi:10.1016/0009-2541(90)90145-W
- Jenson, L.S., 1976, A new method of classifying alkali volcanic rocks: Ontario Division Mineral, Miscellaneous Paper, v. 66, p. 22.
- Jochum, K.P., Arndt, N.T., and Hafmann, A.W., 1991, Nb-Th-La in komatiites and basalts: Constraints on komatiite Petrogenesis and mantle evolution: *Earth Planetary Science Letters*, v. 107, p. 272–289. doi:10.1016/0012-821X(91)90076-T
- Kerr, A.C., White, R.V., and Saunders, A.D., 2000, LIP reading: Recognizing oceanic plateaux in the geological record: *Journal of Petrology*, v. 41, p. 1041–1056. doi:10.1093/petrology/41.7.1041
- Kerrick, R., and Xie, Q., 2002, Compositional recycling structure of an Archaean super-plume: Nb-Th-U-LREE systematics of Archaean Komatiites and basalts revisited: *Contributions to Mineralogy and Petrology*, v. 142, p. 476–484. doi:10.1007/s004100100301
- Kumar, A., Bhaskar Rao, Y.J., Sivaraman, T.V., and Gopalan, K., 1996, Sm-Nd ages of Archaean metavolcanic of the Dharwar craton, South India: *Precambrian Research*, v. 80, p. 206–215. doi:10.1016/S0301-9268(96)00015-0
- Lahaye, X., Arndt, N.T., Byerly, G., Chauvel, C., Fourcade, S., and Gruau, G., 1995, The influence of alteration on the trace-element and Nd isotopic compositions of Komatiites: *Chemical Geology*, v. 126, p. 43–64. doi:10.1016/0009-2541(95)00102-1
- Lecuyer, C., Gruau, G., Anhaeusser, C.R., and Fourcade, S., 1994, The origin of fluids and the effect of metamorphism on the primary chemical compositions of Barberton komatiites; new evidence from geochemical (REE) and isotopic (Nd, O, H, ³⁹Ar/⁴⁰Ar) data: *Geochimica Et Cosmochimica Acta*, v. 58, p. 969–984. doi:10.1016/0016-7037(94)90519-3
- Leshner, C.M., and Arndt, N.T., 1995, REE and Nd isotope geochemistry, petrogenesis and volcanic evolution of contaminated komatiites at Kambalda, Western Australia: *Lithos*, v. 34, p. 127–157. doi:10.1016/0024-4937(95)90017-9
- Lewis, J.D., 1971, Spinifex texture in a slag as evidence for its origin in rocks. Geological Survey of Western Australia Annual Report for 1970. p. 45–49.
- Longerich, H.P., Jenner, G.A., Fryer, B.J., and Jackson, S.E., 1990, Inductively coupled plasma-mass spectrometric analysis of geological samples: A critical evaluation based on case studies: *Chemical Geology*, v. 83, p. 105–118. doi:10.1016/0009-2541(90)90143-U
- Maier, W.D., Peltonen, P., Halkoaho, T., and Hanski, E., 2013, Geochemistry of komatiites from the Tipasjärvi, Kuhmo, Suomussalmi, Ilomantsi and Tulppio greenstone belts, Finland: Implications for tectonic setting and Ni sulphide prospectivity: *Precambrian Research*, v. 228, p. 63–84. doi:10.1016/j.precamres.2012.12.004
- Manikyamba, C., Ganguly, S., Saha, A., Santosh, M., Rajanikanta Singh, M., and Subba Rao, D.V., 2014a, Continental lithospheric evolution: Constraints from the geochemistry of felsic volcanic rocks in the Dharwar Craton, India: *Journal of Asian Earth Sciences*, v. 95, p. 65–80. doi:10.1016/j.jseaes.2014.05.015
- Manikyamba, C., and Kerrich, R.C., 2012, Eastern Dharwar Craton, India: Continental lithosphere growth by accretion of diverse plume and arc terranes: *Geoscience Frontiers*, v. 3, p. 225–240. doi:10.1016/j.gsf.2011.11.009
- Manikyamba, C., Kerrich, R., Polat, A., and Saha, A., 2013, Geochemistry of two stratigraphically-related ultramafic (komatiite) layers from the Neoproterozoic Sigegudda greenstone terrane, Western Dharwar Craton, India: Evidence for compositional diversity in Archean mantle plumes: *Lithos*, v. 177, p. 120–135. doi:10.1016/j.lithos.2013.06.017
- Manikyamba, C., Saha, A., Santosh, M., Ganguly, S., Singh, R., Subba Rao, D.S., and Lingadevaru, M., 2014b, Neoproterozoic felsic volcanic rocks from the Shimoga greenstone belt, Dharwar Craton, India: Geochemical fingerprints of crustal growth at an active continental margin: *Precambrian Research*, v. 252, p. 1–21. doi:10.1016/j.precamres.2014.06.014
- Masuda, A., Nakamura, N., and Tanaka, T., 1973, Fine structure of mutually normalized rare-earth patterns of chondrites:

- Geochimica et Cosmochimica Acta, v. 37, p. 239–248. doi:10.1016/0016-7037(73)90131-2
- Maya, J.M., Bhutani, R., and Balakrishnan, S., 2011, ^{146,147}Sm–^{142,143}Nd studies of komatiites from western Dharwar Craton, India: Implications for depleted mantle evolution in Early Archean. Goldschmidt Conference abstract: Mineralogical Magazine, v. 1430.
- McCuig, T.C., Kerrich, R., and Xie, Q., 1994, Phosphorus and high field strength element anomalies in Archean high-magnesian magmas as possible indicators of source mineralogy and depth: Earth Planetary Science Letters, v. 124, p. 221–239.
- Meen, J.K., Rogers, J.J.W., and Fullagar, P.D., 1992, Lead isotopic compositions in the western Dharwar craton, southern India: Evidence for distinct middle Archean terrains in a late Archean craton: Geochimica Et Cosmochimica Acta, v. 56, p. 2455–2470. doi:10.1016/0016-7037(92)90202-T
- Miller, G.H., Stolper, E.M., and Ahrens, T.J., 1991, The equation of state of molten komatiite. 2. Application to komatiite petrogenesis and the Hadean mantle: Journal of Geophysical Research, v. 96, p. 11849–11864. doi:10.1029/91JB01203
- Mole, D.R., Fiorentini, M.L., Thebaud, N., Cassidy, K.F., McCuig, T., Kirkland, C.L., Romono, S.S., Doublier, M.P., Belusova, E.L., Barnes, S.J., and Miller, J., 2014, Archean komatiite volcanism controlled by evolution of early continents: Proceedings of the National Academy of Sciences. doi:10.1073/pnas.1400273111.
- Mondal, S.K., Mukherjee, R., Rosing, M.T., Frei, R., and Waight, J., 2008, Petrologic, geochemical and isotopic study of 3.1 Ga peridotite-chromite suite from western Dharwar craton (India): Evidence for recycling of oceanic crust in the Mesoarchean. EOS Transactions AGU 89 (53): Fall Meeting Supplementary, v. 33, p. C–2237. Abstract.
- Mukherjee, R., Mondal, S.K., Rosing, M.T., and Robert, F., 2010, Compositional variations in the Mesoarchean chromites of the Nuggihalli schist belt, Western Dharwar Craton (India): Potential parental melts and implications for tectonic setting: Contributions to Mineralogy and Petrology, v. 160, p. 865–885. doi:10.1007/s00410-010-0511-5
- Naqvi, S.M., 1981, The oldest supracrustals of the Dharwar craton, India: Journal of Geological Society of India, v. 22, p. 458–469.
- Naqvi, S.M., Ram Mohan, M., Rana Prathap, J.G., and Srinivasa Sarma, D., 2009, Adakite TTG connection and fate of Mesoarchean basaltic crust of Holenarsipur Nucleus, Dharwar Craton, India: Journal of Asian Earth Sciences, v. 35, p. 416–434. doi:10.1016/j.jseaes.2009.02.005
- Nebel, O., Rapp, R.P., and Yaxley, G.M., 2014, The role of detrital zircons in Hadean crustal research: Lithos, v. 191, p. 313–327. doi:10.1016/j.lithos.2013.12.010
- Nesbit, E.G., Cheadle, M.J., Arndt, N.T., and Bickle, M.J., 1993, Constraining the potential temperature of the Archean mantle: A review of the evidence from komatiites: Lithos, v. 30, p. 291–307. doi:10.1016/0024-4937(93)90042-B
- Nesbitt, R.W., 1971, Skeletal crystal forms in the ultramafic rocks of the Yilgarn Block, Western Australia: Evidence for an Archean ultramafic liquid: Geological Society of Australia (Special Publication), v. 3, p. 331–348.
- Nisbet, E.G., Bickle, M.J., and Martin, A., 1977, The Mafic and Ultramafic Lavas of the Belingwe Greenstone Belt, Rhodesia: Journal of Petrology, v. 18, p. 521–566. doi:10.1093/petrology/18.4.521
- Nutman, A.P., Chadwick, B., Krishna Rao, B., and Vasudev, V.N., 1996, SHRIMP U/Pb zircon ages of acid volcanic rocks in the Chitradurga and Sandur Groups, and granites adjacent to the Sandur schist belt, Karnataka: Journal of the Geological Society of India, v. 47, p. 153–164.
- Nutman, A.P., Chadwick, B., Ramakrishnan, M., and Viswanatha, M.N., 1992, SHRIMP U–Pb ages of detrital zircon in Sargur supracrustal rocks in western Karnataka, southern India: Journal of the Geological Society of India, v. 39, p. 367–374.
- Ohtani, E., Kawabe, I., Moriyama, J., and Nagata, Y., 1989, Partitioning of elements between majorite garnet and melt and implications for petrogenesis of komatiite: Contributions to Mineralogy and Petrology, v. 103, p. 263–269. doi:10.1007/BF00402913
- Paranthaman, S., 2005, Geology and Geochemistry of Archean Ghattihosahalli mafic-ultramafic complex, Chitradurga, Karnataka: Journal of Geological Society of India, v. 66, p. 653–657.
- Parman, S.W., Dann, J.C., Grove, T.L., and De Wit, M.J., 1997, Emplacement conditions of komatiite magmas from the 3.49 Ga Komati formation, Barberton Greenstone Belt, South Africa: Earth and Planetary Science Letters, v. 150, p. 303–323. doi:10.1016/S0012-821X(97)00104-0
- Parman, S.W., Grove, T.L., and Dann, J.C., 2001, The production of Barberton komatiites in an Archean subduction zone: Geophysical Research Letters, v. 38, p. 2513–2516. doi:10.1029/2000GL012713
- Parman, S.W., Grove, T.L., Dann, J.C., and De Wit, M.J., 2004, A subduction origin for komatiites and cratonic lithospheric mantle: South African Journal of Geology, v. 107, p. 107–118. doi:10.2113/107.1-2.107
- Peucat, J.-J., Bouhallier, H., Fanning, C.M., and Jayananda, M., 1995, Age of Holenarsipur schist belt, relationships with the surrounding gneisses (Karnataka, south India): The Journal of Geology, v. 103, p. 701–710. doi:10.1086/629789
- Peucat, J.-J., Jayananda, M., Chardon, D., Capdevila, R., Mark Fanning, C., and Paquette, J.-L., 2013, The lower crust of the Dharwar Craton, Southern India: Patchwork of Archean granulitic domains: Precambrian Research, v. 227, no. 2013, p. 4–28. doi:10.1016/j.precamres.2012.06.009
- Peucat, J.-J., Mahabaleswar, B., and Jayananda, M., 1993, Age of younger tonalitic Magmatism and granulite metamorphism in the south Indian transition zone (Krishnagiri area): Comparison with older peninsular gneisses from Hassan-Gorur area: Journal of Metamorphic Geology, v. 11, p. 879–888. doi:10.1111/j.1525-1314.1993.tb00197.x
- Polat, A., and Kerrich, R., 2000, Archean greenstone belt magmatism and the continental growth-mantle evolution connection: Constraints from Th–U–Nb–LREE systematics of the 2.7 Ga Wawa subprovince, Superior province, Canada: Earth Planetary Science Letters, v. 175, p. 41–54. doi:10.1016/S0012-821X(99)00283-6
- Polat, A., Kerrich, R., and Wyman, D.A., 1999, Geochemical diversity in oceanic komatiites and basalts from the late Archean Wawa greenstone belts, Superior Province, Canada: Trace element and Nd isotope evidence for a heterogeneous mantle: Precambrian Research, v. 94, p. 139–173. doi:10.1016/S0301-9268(98)00110-7
- Prabhakar, B.C., and Namratha, R., 2014, Morphology and textures of komatiite flows of J. C. Pura schist belt, Dharwar

- craton: *Journal of Geological Society of India*, v. 83, p. 13–20. doi:10.1007/s12594-014-0002-9
- Puchtel, I.S., Hasee, K.M., Hofmann, A.W., Chauvel, C., Kulikov, V.S., Garbe Schonberg, C.-D., and Nemchin, A.A., 1997, Petrology and geochemistry of crustally contaminated komatiitic basalts from the Vetryny Belt, south eastern Baltic Shield: Evidence for an early Proterozoic mantle plume beneath rifted Archean continental lithosphere: *Geochimica Et Cosmochimica Acta*, v. 61, p. 1205–1222. doi:10.1016/S0016-7037(96)00410-3
- Pyke, D.R., Naldrett, A.J., and Or, E., 1973, Archean ultramafic flows in Munro Township, Ontario: *Geological Society of America Bulletin*, v. 84, no. 3, p. 955–977. doi:10.1130/0016-7606(1973)84<955:AUFIMT>2.0.CO;2
- Ram Mohan, M., Srinivasa Sarma, D., McNaughton, N., Fletcher, I.R., Wilde, S.A., Siddiqui, M.A., Rasmussen, B., Krapez, B., Gregory, C., and Kamo, S.L., 2014, SHRIMP zircon and titanite U-Pb ages, Lu-Hf isotope signatures and geochemical constraints for ~2.56 Ga granitic magmatism in western Dharwar Craton, southern India: Evidence for short-lived Neoproterozoic crustal growth?: *Precambrian Research*, v. 243, p. 197–220. doi:10.1016/j.precamres.2013.12.017
- Ramakrishnan, M., and Vaidyanadhan, R., 2008, Geology of India: Bangalore, Geological Society of India, 556 p.
- Ramakrishnan, M., Venkata Dasu, S.P., and Kroner, A., 1994, Middle Archean age of Sargur Group by single grain zircon dating and geochemical evidence for the clastic origin of metaquartzite from J.C. Pura greenstone belt, Karnataka: *Journal of the Geological Society of India*, v. 44, p. 605–616.
- Rollinson, H.R., Windley, B.F., and Ramakrishnan, M., 1981, Contrasting high and intermediate pressures of metamorphism in the Archean Sargur Schists of southern India: *Contribution to Mineralogy and Petrology*, v. 76, p. 420–429. doi:10.1007/BF00371484
- Roth, A.S.G., Bourdon, B., Mojzsis, S.J., Touboul, M., Sprung, P., Guitreau, M., and Blichert-Toft, J., 2013, Inherited ¹⁴²Nd anomalies in Eoarchean protoliths: *Earth and Planetary Science Letters*, v. 361, p. 50–57. doi:10.1016/j.epsl.2012.11.023
- Santosh, M., Yang, Q.-Y., Shaji, E., Tsunogae, T., Ram Mohan, M., and Satyanarayanan, M., 2015, An exotic Mesoarchean microcontinent: The Coorg Block, southern India: *Gondwana Research*, v. 27, p. 165–195. doi:10.1016/j.gr.2013.10.005
- Sarma, S.D., McNaughton, N.J., Elena, B., Ram Mohan, M., and Fletcher, I.R., 2012, Detrital zircon U–Pb ages and Hf-isotope systematics from the Gadag Greenstone Belt: Archean crustal growth in the western Dharwar Craton: *India. Gondwana Research*, v. 22, no. 3–4, p. 843–854. doi:10.1016/j.gr.2012.04.001
- Saunders, A.D., Norry, M.J., and Tarney, J., 1988, Origin of MORB and chemically-depleted mantle reservoirs: Trace element constraints, in Menzies, M.A., and Cox, K.G., eds., *Oceanic and continental lithosphere: Similarities and differences*: London, Oxford university press, 415–445 p.
- Shore, M., 1996, Cooling and crystallization of komatiite flows. [Ph.D. thesis]: Ottawa, National Library of Canada, P 244.
- Shore, M., and Fowler, A.D., 1999, The origin of spinifex texture in komatiites: *Nature*, v. 387, p. 691–693.
- Smith, H.S., Erlank, A.J., and Duncan, A.R., 1980, Geochemistry of some ultramafic komatiite lava flows from the Barberton Mountain Land, South Africa: *Precambrian Research*, v. 11, p. 399–415. doi:10.1016/0301-9268(80)90074-1
- Srikantia, S.V., and Bose, S.S., 1985, Archean komatiites from banasandra area of kibbanahalli arm of chitradurga supra-crustal belt in Karnataka: *Journal of Geological Society of India*, v. 26, p. 407–417.
- Srikantia, S.V., and Rao, M.S., 1990, Unusual concentric structure in komatiite of kibbanahalli arm of chitradurga supra-crustal belt near Banasandra, Karnataka: *Journal of Geological Society of India*, v. 36, p. 424–429.
- Srikantia, S.V., and Venkataramana, P., 1989, The Archean komatiites of Nagamangala supracrustal belt, Karnataka: *Journal of Geological Society of India*, v. 33, p. 210–214.
- Subba Rao, D.V., and Naqvi, S.M., 1999, Archean Komatiites from the older schist belt of Kalyadi in Western Dharwar Craton, Karnataka: *Journal of Geological Society of India*, v. 53, p. 347–354.
- Sun, S., and McDonough, W., 1989, Chemical and isotopic systematics of oceanic basalts: Implications for mantle composition and processes, in Saunders, A.D., and Norry, M.J., eds., *Magmatism in the Ocean Basins*: London, England, Geological Society of London, 313–345 p.
- Sun, -S.-S., and Nesbitt, R.W., 1978, Petrogenesis of Archean ultrabasic and basic volcanics: Evidence from rare earth elements: *Contributions to Mineralogy and Petrology*, v. 65, p. 301–325. doi:10.1007/BF00375516
- Swami Nath, J., and Ramakrishnan, M., 1981, Early Precambrian supracrustals of southern Karnataka: *Memoir Geological Survey of India*, v. 112, p. 350.
- Swami Nath, J., Ramakrishnan, M., and Viswanatha, M.N., 1976, Dharwar stratigraphic model and Karnataka craton evolution: *Geological Survey of India Records*, v. 107, p. 149–175.
- Taylor, S.R., and Gordon, M.P., 1977, Geochemical application of spark source mass spectrometry. III. Element sensitivity, precision and accuracy: *Geochimica Et Cosmochimica Acta*, v. 41, p. 1375–1380. doi:10.1016/0016-7037(77)90080-1
- Tourpin, S., Gruau, G., Blais, S., and Fourcade, S., 1991, Resetting of REE, and Nd and Sr isotopes during carbonitisation of a Komatiite flow from Finland: *Chemical Geology*, v. 90, p. 15–29. doi:10.1016/0009-2541(91)90030-U
- Trendall, A.F., De Laeter, J.R., Nelson, D.R., and Mukhopadhyay, D., 1997, A precise U-Pb age for the base of Mulaingiri formation (Bababudan Group, Dharwar Supergroup) of the Karnataka craton: *Journal of Geological Society of India*, v. 50, p. 161–170.
- Tushipokla, and Jayananda, M., 2013, Geochemical constraints on komatiite volcanism from Sargur Group Nagamangala greenstone belt, western Dharwar craton, southern India: Implications for Mesoarchean mantle evolution and continental growth: *Geoscience Frontiers*, v. 4, p. 321–340. doi:10.1016/j.gsf.2012.11.003
- Venkata Dasu, S.P., Ramakrishnan, M., and Mahabaleswar, B., 1991, Sargur–Dharwar relationship around the komatiite-rich J.C. Pura greenstone belt in Karnataka: *Journal of the Geological Society of India*, v. 38, p. 577–592.
- Viljoen, M.J., Viljoen, R.P., and Pearton, T.N., 1982, The nature and distribution of Archean komatiite volcanics in South Africa, in Arndt, N.T., and Nisbet, E.G., eds., *Komatiites*: London, Allen and Unwin, 53–79 p.
- Viljoen, R.P., and Viljoen, M.J., 1969, The geology and geochemistry of the lower ultramafic unit of the Onverwacht Group and a proposed new class of igneous rocks:

- Geological Society of South Africa, Special Publication, v. 21, p. 55–85.
- Viljoen, R.P., Viljoen, M.J., Smith, H.S., and Erlank, A.J., 1983, Geological, textural and geochemical features of komatiitic flows from the Komati Formation: Geological Society of South Africa Special Publication, v. 9, p. 1–20.
- Williams, D.A.C., and Furnell, R.G., 1979, Reassessment of part of the Barberton type area, South Africa: Precambrian Research, v. 9, p. 325–347. doi:10.1016/0301-9268(79)90011-1
- Xie, Q., Kerrich, R., and Fan, J., 1993, HFSE/REE fractionation recorded in three Komatiite-basalt sequences, Archaean Abitibi green stone belt: Implication for multiple plume sources and depths: Geochimica Et Cosmochimica Acta, v. 57, p. 4111–4411. doi:10.1016/0016-7037(93)90357-3

Appendix

Analytical methods

The least altered samples were selected for geochemical studies. Rocks were chipped into smaller pieces and powdered using a jaw-crusher and agate mortar, at the Department of Geology, Centre for Advanced Studies, University of Delhi, to obtain powder of 60–80 mesh size and ultimately 200 mesh size using an agate mill. A total of 66 samples were selected for major, trace element, and REE analysis. Pressed pellets were produced for determination of major elements by X-ray fluorescence spectrometry (XRF, Philips 1400) at the University of Delhi. These were prepared by thoroughly mixing half a spoonful of 200-mesh powder with binder (polyvinyl alcohol) in an agate mortar and then pressing under hydraulic pressure of about 15,000 kg/cm². Major elements

were determined in pressed pellets by XRF (Pan Analytical Axios Model PW4400/40) at the Department of Geology, University of Delhi. The precision for major elements is as follows: SiO₂, 1%; Al₂O₃, 1.5–3%; Fe₂O₃, 2–3%; MnO, 10%; MgO, 1–3%; CaO, 2–5%; Na₂O, 1.5–3%; K₂O, 2.5%; TiO₂, 2–5%; P₂O₅, 5%.

Trace elements, including REEs, were analysed by ICP-MS (Perkin Elmer SCIEX ELAN DRC II) at the National Geophysical Research Institute (NGRI), India following the procedures described by Jenner *et al.* (1990), Longrich *et al.* (1990), and Balaram and Ganeswar Rao (2003). The following dissolution method was employed. A mixture of double-distilled acids (HF + HNO₃ + HCl, 5:3:2) was added to ca. 50 mg rock powder in Savillex vessels and kept on a hot plate at 150°C for three days. Following this, the entire mixture was evaporated to dryness. The decomposition procedure was repeated by adding 5 ml of the above acid mixture for two days. When the sample was dry, 10 ml of 1:1 HNO₃ was added and heated at 150°C for 10–15 min, then 5 ml Rh (1 ppm concentration) was added as an internal standard. After cooling, the volume of the solution was made up to 250 ml. JA-1 and JR-1 were used as reference materials. For trace elements, precision was better than 5%; for elements with concentration less than 30 ppm the uncertainty was within 10%, and for those with concentration less than 5 ppm it was in the range 10–50%. The international reference materials used at the NGRI ICP-MS laboratory included BHVO-1 and JR-1. The lower detection limit for most trace elements, including REEs, was less than 0.02 ng/L. Chondrite-normalized ratios were calculated using Leedy chondrite values, and primitive mantle-normalized ratios were calculated from the values of Sun and McDonough (1989).